Journal of Computational Mathematics
Vol.xx, No.x, 2024, 1–35.
http://www.global-sci.org/jcm
doi:10.4208/jcm.2310-m2022-0141

UNIFORM ERROR BOUNDS OF AN ENERGY-PRESERVING EXPONENTIAL WAVE INTEGRATOR FOURIER PSEUDO-SPECTRAL METHOD FOR THE NONLINEAR SCHRÖDINGER EQUATION WITH WAVE OPERATOR AND WEAK NONLINEARITY*

Jiyong Li
School of Mathematics Science, Hebei Normal University, Hebei Key Laboratory of Computational Mathematics and Applications, Shijiazhuang 050024, China
Email: ljyong406@163.com

Abstract

Recently, the numerical methods for long-time dynamics of PDEs with weak nonlinearity have received more and more attention. For the nonlinear Schrödinger equation (NLS) with wave operator (NLSW) and weak nonlinearity controlled by a small value $\varepsilon \in (0,1]$, an exponential wave integrator Fourier pseudo-spectral (EWIFP) discretization has been developed (Guo et al., 2021) and proved to be uniformly accurate about ε up to the time at $\mathcal{O}(1/\varepsilon^2)$. However, the EWIFP method is not time symmetric and can not preserve the discrete energy. As we know, the time symmetry and energy-preservation are the important structural features of the true solution and we hope that this structure can be inherited along the numerical solution. In this work, we propose a time symmetric and energy-preserving exponential wave integrator Fourier pseudo-spectral (SEPEWIFP) method for the NLSW with periodic boundary conditions. Through rigorous error analysis, we establish uniform error bounds of the numerical solution at $\mathcal{O}(h^{m_0}+\varepsilon^{2-\beta}\tau^2)$ up to the time at $\mathcal{O}(1/\varepsilon^{\beta})$ for $\beta \in [0,2]$, where h and τ are the mesh size and time step, respectively, and m_0 depends on the regularity conditions. The tools for error analysis mainly include cut-off technique and the standard energy method. We also extend the results on error bounds, energy-preservation and time symmetry to the oscillatory NLSW with wavelength at $\mathcal{O}(\varepsilon^2)$ in time which is equivalent to the NLSW with weak nonlinearity. Numerical experiments confirm that the theoretical results in this paper are correct. Our method is novel because that to the best of our knowledge there has not been any energy-preserving exponential wave integrator method for the NLSW.

Mathematics subject classification: 35Q55, 65M12, 65M15, 65M70, 81-08.
Key words: Nonlinear Schrödinger equation with wave operator and weak nonlinearity, Fourier pseudo-spectral method, Exponential wave integrator, Energy-preserving method, Error estimates, Oscillatory problem.

1. Introduction

In this paper, we consider the following nonlinear Schrödinger equation with wave operator in d $(d=1,2,3)$ dimensions on a torus $\mathbb{T}^d$:

$$\begin{cases} i\partial_t u(\mathbf{x},t)-\alpha\partial_{tt}u(\mathbf{x},t)+\Delta u(\mathbf{x},t)-\varepsilon^2|u(\mathbf{x},t)|^2u(\mathbf{x},t)=0, & \mathbf{x}\in\mathbb{T}^d, \quad t>0, \\ u(\mathbf{x},0)=u_0(\mathbf{x}), \quad \partial_t u(\mathbf{x},0)=u_1(\mathbf{x}), & \mathbf{x}\in\mathbb{T}^d, \end{cases} \tag{1.1}$$

* Received May 29, 2022 / Revised version received March 13, 2023 / Accepted October 1, 2023 / Published online January 15, 2024 /

where $\mathbf{x} \in \mathbb{T}^d$ is the spatial coordinate, t is time, Δ is Laplacian, $\alpha > 0, u := u(\mathbf{x}, t)$ is a complex-valued scalar field, $\varepsilon \in (0, 1]$ is a dimensionless parameter characterizing the nonlinear strength, the functions $u_0(\mathbf{x})$ and $u_1(\mathbf{x})$ are complex-valued and independent of ε [2,6,11,15,34,35,37,39]. The NLSW (1.1) has different physical applications, including the nonrelativistic limit of the Klein-Gordon (KG) equation [34,35,37], the Langmuir wave envelope approximation in plasma [11, 15], and the modulated planar pulse approximation of the sine-Gordon equation for light bullets [6, 39]. The NLSW (1.1) is time symmetric and preserves the mass and the energy as

$$\begin{aligned} M(t) &:= \int_{\mathbb{T}^d} |u(\mathbf{x}, t)|^2 \mathrm{d}\mathbf{x} - 2\alpha \int_{\mathbb{T}^d} \mathrm{Im}\left[\overline{u(\mathbf{x}, t)} \partial_t u(\mathbf{x}, t)\right] \mathrm{d}\mathbf{x} := M(0), \quad t \geq 0, \\ E(t) &:= \int_{\mathbb{T}^d} \left[\alpha |\partial_t u(\mathbf{x}, t)|^2 + |\nabla u(\mathbf{x}, t)|^2 + \frac{1}{2}\varepsilon^2 |u(\mathbf{x}, t)|^4\right] \mathrm{d}\mathbf{x} := E(0), \quad t \geq 0, \end{aligned} \tag{1.2}$$

where $\overline{c}$ and $\mathrm{Im}(c)$ denote the conjugate and imaginary part of c, respectively.

By introducing $w(\mathbf{x}, t) = \varepsilon u(\mathbf{x}, t)$, we can reformulate the NLSW (1.1) with weak nonlinearity as the following NLSW with small initial data at $\mathcal{O}(\varepsilon)$:

$$\begin{cases} i\partial_t w(\mathbf{x}, t) - \alpha \partial_{tt} w(\mathbf{x}, t) + \Delta w(\mathbf{x}, t) - |w(\mathbf{x}, t)|^2 w(\mathbf{x}, t) = 0, & \mathbf{x} \in \mathbb{T}^d, \quad t > 0, \\ w(\mathbf{x}, 0) = \varepsilon u_0(\mathbf{x}), \quad \partial_t w(\mathbf{x}, 0) = \varepsilon u_1(\mathbf{x}), & \mathbf{x} \in \mathbb{T}^d. \end{cases} \tag{1.3}$$

Again, the above NLSW (1.3) is time symmetric and preserves the mass and the energy as

$$\begin{aligned} \widetilde{M}(t) &:= \int_{\mathbb{T}^d} |w(\mathbf{x}, t)|^2 \mathrm{d}\mathbf{x} - 2\alpha \int_{\mathbb{T}^d} \mathrm{Im}\left[\overline{w(\mathbf{x}, t)} \partial_t w(\mathbf{x}, t)\right] \mathrm{d}\mathbf{x} := \widetilde{M}(0), \quad t \geq 0, \\ \widetilde{E}(t) &:= \int_{\mathbb{T}^d} \left[\alpha |\partial_t w(\mathbf{x}, t)|^2 + |\nabla w(\mathbf{x}, t)|^2 + \frac{1}{2} |w(\mathbf{x}, t)|^4\right] \mathrm{d}\mathbf{x} := \widetilde{E}(0), \quad t \geq 0. \end{aligned} \tag{1.4}$$

Due to that the Eqs. (1.1) and (1.3) are equivalent, in the following, we only present numerical methods and related analysis for the NLSW (1.1) with weak nonlinearity. For the NLSW (1.3) with small initial data, the formulation of the new method and the analysis process are completely similar.

When $\alpha = 0$, the NLSW (1.1) reduces to the nonlinear Schrödinger equation. There are various numerical methods for NLS in the literature, including the time-splitting pseudospectral method [3, 10, 12, 16, 26, 33], the finite difference method [1, 3, 4, 13], etc. Meanwhile, for fixed $\varepsilon = 1$, there are some numerical methods for the NLSW, such as conservative finite difference methods [14, 15, 23, 28, 38] and exponential wave integrator method [2, 5]. Conservative finite difference methods are very popular due to that they can preserve the discrete energy and mass. In the recent work [2, 5], two finite difference methods (CNFD and SIFD) and an exponential wave integrator sine pseudospectral (EWISP) method have been analyzed for NLSW with $\alpha \to 0, \varepsilon = 1$ and proved to have different uniform error estimates with respect to $\alpha \in (0, 1]$ for well-prepared initial data and for ill-prepared initial data, respectively. For the research on numerical methods of NLSW in other parameter regimes, we see [40].

Recently, the numerical methods for long-time dynamics of PDEs with weak nonlinearity have received more and more attention. The long-time dynamics of the Klein-Gordon (KG) equations and Dirac equations with weak nonlinearity or small potential are thoroughly studied in the literature [7, 8, 18, 20–22, 30–32]. For the weak nonlinear NLSW with periodic boundary condition, an exponential wave integrator Fourier pseudo-spectral method has been proposed in [24] and proved to be uniformly accurate about ε up to the time at $\mathcal{O}(1/\varepsilon^2)$. Numerical experiments show that the solutions of the EWIFP method have good numerical accuracy and stability. However, the EWIFP method can not preserve the discrete energy. In addition, the time symmetry of the EWIFP method is not considered. It is well known that the energy-conservation and time symmetry are considered very important structures of the NLSW [25]. To the best of my knowledge there is no energy-preserving exponential wave integrator method for the NLSW (1.1).

In this work, we propose a time symmetric and energy-preserving exponential wave integrator Fourier pseudo-spectral method for the NLSW with periodic boundary conditions. By carrying out a rigourously error analysis, we establish error bounds for the SEPEWIFP method at $\mathcal{O}(h^{m_0} + \varepsilon^{2-\beta}\tau^2)$ up to the time at $\mathcal{O}(1/\varepsilon^{\beta})$ for $\beta \in [0, 2]$, where h and τ are the mesh size and time step, respectively and m_0 depends on the regularity conditions. We also extend the results on error bounds, energy-preservation and time symmetry to the oscillatory NLSW which is equivalent to the NLSW with weak nonlinearity.

The framework of this paper is as follows. In Section 2, we propose the SEPEWIFP method for the NLSW (1.1) with periodic boundary conditions. Section 3 introduces some important lemmas and then shows that the method is time symmetric and unique solvable. The method is proved to be energy-preserving in Section 4. In Section 5, we establish rigorous error bounds of the numerical solution for the method applied to the NLSW (1.1) up to the time at $\mathcal{O}(1/\varepsilon^2)$. Section 6 presents the numerical experiments which confirm that the theoretical results in this paper are correct. In Section 7, we extend the results on error bounds, energy-preservation and time symmetry to an oscillatory NLSW. Finally, we draw some conclusions and give a brief discussion about our future work in the last section. Throughout this paper, we take the notation $p \lesssim q$ to represent that there exists a generic constant $C > 0$ independent of h, τ and ε such that $|p| \le Cq$.

2. Derivation of the New Method

For convenience, we only consider the 1D problem. For high-dimensional problems, the method, the proof of the structure preservation, and the error analysis are all similar. In 1D, the NLSW (1.1) with periodic boundary conditions collapses to

$$\begin{aligned} &i\partial_t u(x,t) - \alpha\partial_{tt}u(x,t) + \Delta u(x,t) - \varepsilon^2|u(x,t)|^2 u(x,t) = 0, && x \in \Omega = (a,b), \quad t > 0, \\ &u(x,0) = u_0(x), \quad \partial_t u(x,0) = u_1(x), && x \in \overline{\Omega} = [a,b], \\ &u(a,t) = u(b,t), \quad \partial_x u(a,t) = \partial_x u(b,t), && t \ge 0. \end{aligned} \tag{2.1}$$

For brevity, we use the notation

$$G(u) = |u|^2 u. \tag{2.2}$$

For $\Omega = [a,b]$, we denote by $H^m(\Omega)$ with integer $m \ge 0$, the standard Sobolev space and express the corresponding norm as

$$\|f\|_m^2 = \sum_{l \in Z}(1 + |\mu_l|^2)^m \big|\hat{f}_l\big|^2, \quad f(x) = \sum_{l \in Z} \hat{f}_l e^{i\mu_l(x-a)}, \quad \mu_l = \frac{2\pi l}{b-a}. \tag{2.3}$$

Choose the mesh size $h := \Delta x = (b-a)/M$ with M a positive even integer, time step $\tau := \Delta t > 0$ and denote grid points as $x_j := a + jh$ for $j = 0, 1, \ldots, M$, $t_n := n\tau$ for $n = 0, 1, \ldots$. Let

$$\begin{aligned} &Y_M := \operatorname{span}\left\{ \mathrm{e}^{i\mu_l(x-a)} \,\middle|\, \mu_l = \frac{2\pi l}{b-a},\ l \in \Omega_M \right\}, \\ &X_M := \operatorname{span}\left\{ v = (v_0, \cdots, v_M) \,|\, v_0 = v_M \right\} \in \mathbb{C}^{M+1}, \end{aligned} \tag{2.4}$$

where

$$\Omega_M = \left\{ l \,|\, l = -\frac{M}{2}, \cdots, \frac{M}{2} - 1 \right\}.$$

For any periodic function $v(x)$ on $[a,b]$ and vector $v \in X_M$, define $P_M : L^2(a,b) \to Y_M$ as the standard projection operator, $I_M : C(a,b) \to Y_M$ and $I_M : X_M \to Y_M$ as the trigonometric interpolation operators [36], i.e.

$$(P_M v)(x) = \sum_{l\in\Omega_M} \widehat{v}_l \mathrm{e}^{i\mu_l(x-a)}, \quad (I_M v)(x) = \sum_{l\in\Omega_M} \widetilde{v}_l \mathrm{e}^{i\mu_l(x-a)}, \quad x \in [a,b] \tag{2.5}$$

with $l \in \Omega_M$ and the coefficients

$$\widehat{v}_l = \frac{1}{b-a}\int_a^b v(x)\mathrm{e}^{-i\mu_l(x-a)}\mathrm{d}x, \quad \widetilde{v}_l = \frac{1}{M}\sum_{j=0}^{M-1} v_j \mathrm{e}^{-i\mu_l(x_j-a)}, \tag{2.6}$$

respectively, where $v_j{=}v(x_j)$ for the case where $v(x)$ is a periodic function satisfying $v(a){=}v(b)$. The Fourier spectral method for solving (2.1) is finding $u_M(x,t) \in Y_M$, i.e.

$$u_M(x,t) = \sum_{l\in\Omega_M} \widehat{(u_M)}_l(t)\mathrm{e}^{i\mu_l(x-a)}, \quad x \in [a,b], \quad t \geq 0, \tag{2.7}$$

satisfying

$$i\partial_t u_M - \alpha\partial_{tt}u_M + \partial_{xx}u_M - \varepsilon^2 P_M G(u_M) = 0, \quad x \in [a,b], \quad t \geq 0. \tag{2.8}$$

Plugging (2.7) into (2.8) and using the orthogonality of $\mathrm{e}^{i\mu_l(x-a)}$ for $l \in \Omega_M$, we find

$$i\frac{\mathrm{d}}{\mathrm{d}t}\widehat{(u_M)}_l(t) - \alpha\frac{\mathrm{d}^2}{\mathrm{d}t^2}\widehat{(u_M)}_l(t) - |\mu_l|^2\widehat{(u_M)}_l(t) - \varepsilon^2\widehat{G(u_M)}_l(t) = 0, \quad l \in \Omega_M, \quad t \geq 0. \tag{2.9}$$

After a simple arrangement, we obtain

$$\frac{\mathrm{d}^2}{\mathrm{d}t^2}\widehat{(u_M)}_l(t) = \frac{i}{\alpha}\frac{\mathrm{d}}{\mathrm{d}t}\widehat{(u_M)}_l(t) - \frac{|\mu_l|^2}{\alpha}\widehat{(u_M)}_l(t) - \frac{\varepsilon^2}{\alpha}\widehat{G(u_M)}_l(t), \quad l \in \Omega_M, \quad t \geq 0. \tag{2.10}$$

For $l \in \Omega_M$, we denote

$$a_l = \sqrt{1 + 4\alpha|\mu_l|^2}. \tag{2.11}$$

From the variation-of-constants formula, we know that

$$\begin{aligned}
\widehat{(u_M)}_l(t_n{+}s) &= A_l(s)\widehat{(u_M)}_l(t_n) + B_l(s)\widehat{(\dot{u}_M)}_l(t_n) - \frac{\varepsilon^2}{\alpha}\int_0^s B_l(s-z)\widehat{G(u_M)}_l(t_n{+}z)\mathrm{d}z, \\
\widehat{(\dot{u}_M)}_l(t_n{+}s) &= C_l(s)\widehat{(u_M)}_l(t_n) + D_l(s)\widehat{(\dot{u}_M)}_l(t_n) - \frac{\varepsilon^2}{\alpha}\int_0^s D_l(s-z)\widehat{G(u_M)}_l(t_n{+}z)\mathrm{d}z,
\end{aligned} \tag{2.12}$$

where $\dot{u}_M(x,t_n) = \partial_t u_M(x,t_n)$ and

$$\begin{aligned}
A_l(s) &= \mathrm{e}^{\frac{is}{2\alpha}}\left(\cos\left(\frac{sa_l}{2\alpha}\right) - \frac{i}{a_l}\sin\left(\frac{sa_l}{2\alpha}\right)\right), \quad && B_l(s) = \mathrm{e}^{\frac{is}{2\alpha}}\frac{2\alpha}{a_l}\sin\left(\frac{sa_l}{2\alpha}\right), \\
C_l(s) &= -\mathrm{e}^{\frac{is}{2\alpha}}\frac{2\mu_l^2}{a_l}\sin\left(\frac{sa_l}{2\alpha}\right), && D_l(s) = \mathrm{e}^{\frac{is}{2\alpha}}\left(\cos\left(\frac{sa_l}{2\alpha}\right) + \frac{i}{a_l}\sin\left(\frac{sa_l}{2\alpha}\right)\right).
\end{aligned} \tag{2.13}$$

In order to construct an energy-preseving method, we define the functions $P_l(s)$ and $Q_l(s)$ as

$$P_l(s) = \int_0^s B_l(s-z)\mathrm{d}z, \quad Q_l(s) = \int_0^s D_l(s-z)\mathrm{d}z. \tag{2.14}$$

The functions $P_l(s)$ and $Q_l(s)$ are continuous with respect to s. Direct calculation gives

$$\begin{aligned} P_l(s) &= \begin{cases} \dfrac{\alpha}{\mu_l^2}\left(1-\mathrm{e}^{\frac{is}{2\alpha}}\left(\cos\left(\dfrac{sa_l}{2\alpha}\right)-\dfrac{i}{a_l}\sin\left(\dfrac{sa_l}{2\alpha}\right)\right)\right), & \mu_l\neq 0,\\ \alpha\big(\alpha-\alpha\mathrm{e}^{\frac{is}{\alpha}}+is\big), & \mu_l=0, \end{cases} \\ Q_l(s) &= \mathrm{e}^{\frac{is}{2\alpha}}\frac{2\alpha}{a_l}\sin\left(\frac{sa_l}{2\alpha}\right). \end{aligned} \tag{2.15}$$

Using the functions (2.14) and taking $s=\tau$ in (2.12), we approximate the integrals as follows:

$$\begin{aligned} &\int_0^\tau B_l(\tau-z)\widehat{G(u_M)}_l(t_n+z)\mathrm{d}z \approx P_l(\tau)\widehat{G\Big(u_M(x,t_{n+1}),u_M(x,t_n)\Big)}_l,\\ &\int_0^\tau D_l(\tau-z)\widehat{G(u_M)}_l(t_n+z)\mathrm{d}z \approx Q_l(\tau)\widehat{G\Big(u_M(x,t_{n+1}),u_M(x,t_n)\Big)}_l, \end{aligned} \tag{2.16}$$

where

$$\begin{aligned} G\big(u_M(x,t_{n+1}),u_M(x,t_n)\big) = \frac{1}{4}&\left(|u_M(x,t_{n+1})|^2+|u_M(x,t_n)|^2\right)\\ &\times\big(u_M(x,t_{n+1})+u_M(x,t_n)\big). \end{aligned} \tag{2.17}$$

In practice, because that computing $\widehat{(u_M)}_l$ in (2.6) is difficult, we approximate it by the numerical quadratures defined in (2.6). Let u_j^n and $\dot{u}_j^n$ $(j=0,\ldots,M)$ be the approximations of $u(x_j,t_n)$ and $\partial_t u(x_j,t_n)$, respectively. Choose $u_j^0=u_0(x_j)$ and $\dot{u}_j^0=u_1(x_j)$, then for $n=0,1,\ldots,$ a time symmetric and energy-preserving exponential wave integrator Fourier pseudo-spectral discretization for (2.1) is

$$u_j^{n+1}=\sum_{l\in\Omega_M}\widetilde{(u^{n+1})}_l\mathrm{e}^{\frac{2ijl\pi}{M}},\quad \dot{u}_j^{n+1}=\sum_{l\in\Omega_M}\widetilde{(\dot{u}^{n+1})}_l\mathrm{e}^{\frac{2ijl\pi}{M}}, \tag{2.18}$$

where

$$\widetilde{(u^{n+1})}_l = A_l(\tau)\widetilde{(u^n)}_l + B_l(\tau)\widetilde{(\dot{u}^n)}_l - \frac{\varepsilon^2}{\alpha}P_l(\tau)\widetilde{G(u^{n+1},u^n)}_l, \tag{2.19}$$

$$\widetilde{(\dot{u}^{n+1})}_l = C_l(\tau)\widetilde{(u^n)}_l + D_l(\tau)\widetilde{(\dot{u}^n)}_l - \frac{\varepsilon^2}{\alpha}Q_l(\tau)\widetilde{G(u^{n+1},u^n)}_l \tag{2.20}$$

with $G(u^{n+1},u^n)_j$ given as

$$G(u^{n+1},u^n)_j=\frac{1}{4}\big(|u_j^{n+1}|^2+|u_j^n|^2\big)\big(u_j^{n+1}+u_j^n\big). \tag{2.21}$$

Remark 2.1. In the papers [19, 24], the authors applied the variation-of-constants formula to (2.10) and then get another integral equation that looks different form our integral equation (2.12). In fact, the two integral equations are essentially equivalent to each other.

3. Time Symmetry and Unique Solvability

In this section we study the time symmetry and unique solvability of the SEPEWIFP method. The following lemmas are useful.

Lemma 3.1. *For the coefficients in* (2.13)*, the following relationship is established:*

$$\begin{pmatrix} A_l(-\tau) & B_l(-\tau) \\ C_l(-\tau) & D_l(-\tau) \end{pmatrix}^{-1} = \begin{pmatrix} A_l(\tau) & B_l(\tau) \\ C_l(\tau) & D_l(\tau) \end{pmatrix}, \quad l \in \Omega_M. \tag{3.1}$$

Proof. Obviously, we just need to prove for $l \in \Omega_M$,

$$\begin{pmatrix} A_l(-\tau) & B_l(-\tau) \\ C_l(-\tau) & D_l(-\tau) \end{pmatrix} \begin{pmatrix} A_l(\tau) & B_l(\tau) \\ C_l(\tau) & D_l(\tau) \end{pmatrix} = \begin{pmatrix} 1 & 0 \\ 0 & 1 \end{pmatrix}. \tag{3.2}$$

Firstly, we prove that the elements of the first row and first column of the two matrices on two side of (3.2) are equal. Direct calculation gives

$$\begin{aligned} & A_l(-\tau)A_l(\tau) + B_l(-\tau)C_l(\tau) \\ =& \left(\cos\left(\frac{sa_l}{2\alpha}\right) - \frac{i}{a_l}\sin\left(\frac{sa_l}{2\alpha}\right)\right)\left(\cos\left(\frac{sa_l}{2\alpha}\right) + \frac{i}{a_l}\sin\left(\frac{sa_l}{2\alpha}\right)\right) - \frac{4\alpha\mu^2}{a_l^2}\sin^2\left(\frac{sa_l}{2\alpha}\right) \\ =& \left(\cos^2\left(\frac{sa_l}{2\alpha}\right) + \frac{1}{a_l^2}\sin^2\left(\frac{sa_l}{2\alpha}\right)\right) - \frac{4\alpha\mu^2}{a_l^2}\sin^2\left(\frac{sa_l}{2\alpha}\right) = 1. \end{aligned} \tag{3.3}$$

The equality of other elements can be proved similarly. □

Lemma 3.2. *For the coefficients in* (2.13)*, the following relationship is established:*

$$\operatorname{Re} P_l^{-1}(\tau) > 0, \quad \tau \neq 2k\pi\alpha, \tag{3.4}$$

where $l \in \Omega_M$ *and* k *is arbitrary integer.*

Proof. From the fact that for $\mu_l \neq 0$ and $s \neq 0$,

$$\begin{aligned} \left| e^{\frac{is}{2\alpha}}\left(\cos\left(\frac{sa_l}{2\alpha}\right) - \frac{i}{a_l}\sin\left(\frac{sa_l}{2\alpha}\right)\right)\right| &= \left|\cos\left(\frac{sa_l}{2\alpha}\right) - \frac{i}{a_l}\sin\left(\frac{sa_l}{2\alpha}\right)\right| \\ &= \sqrt{\cos^2\left(\frac{sa_l}{2\alpha}\right) + \frac{1}{a_l^2}\sin^2\left(\frac{sa_l}{2\alpha}\right)} < 1, \end{aligned} \tag{3.5}$$

we have for any step size $\tau(\neq 0)$ and $\mu_l \neq 0$,

$$\begin{aligned} \operatorname{Re} P_l(\tau) &= \frac{\alpha}{\mu_l^2}\operatorname{Re}\left(1 - e^{\frac{is}{2\alpha}}\left(\cos\left(\frac{sa_l}{2\alpha}\right) - \frac{i}{a}\sin\left(\frac{sa_l}{2\alpha}\right)\right)\right) \\ &= \frac{\alpha}{\mu_l^2}\left(1 - \operatorname{Re}\left[e^{\frac{is}{2\alpha}}\left(\cos\left(\frac{sa_l}{2\alpha}\right) - \frac{i}{a}\sin\left(\frac{sa_l}{2\alpha}\right)\right)\right]\right) \\ &\geq \frac{\alpha}{\mu_l^2}\left(1 - \left|e^{\frac{is}{2\alpha}}\left(\cos\left(\frac{sa_l}{2\alpha}\right) - \frac{i}{a}\sin\left(\frac{sa_l}{2\alpha}\right)\right)\right|\right) > 0. \end{aligned} \tag{3.6}$$

For $\mu_l = 0$, we have for $\tau \neq 2k\pi\alpha$,

$$\operatorname{Re} P_l(\tau) = \operatorname{Re}\left(1 - e^{\frac{i\tau}{\alpha}}\right)\alpha^2 = 1 - \cos\left(\frac{\tau}{\alpha}\right) > 0. \tag{3.7}$$

The results (3.6) and (3.7) imply the result (3.4). □

For the time symmetry of the SEPEWIFP method, we have theorem.

Theorem 3.1. *The SEPEWIFP method is time symmetric, i.e. interchanging $u^{n+1}, \dot{u}^{n+1}$ and τ with $u^n, \dot{u}^n$ and $-\tau$, respectively, the method remains unchanged.*

Proof. Exchanging $(u^{n+1}, \dot{u}^{n+1}, \tau) \leftrightarrow (u^n, \dot{u}^n, -\tau)$ in (2.19) and (2.20) results in

$$\begin{aligned}\widetilde{(u^n)}_l &= A_l(-\tau)\widetilde{(u^{n+1})}_l + B_l(-\tau)\widetilde{(\dot{u}^{n+1})}_l - \frac{\varepsilon^2}{\alpha}P_l(-\tau)G\widetilde{(u^{n+1}, u^n)}_l,\\ \widetilde{(\dot{u}^n)}_l &= C_l(-\tau)\widetilde{(u^{n+1})}_l + D_l(-\tau)\widetilde{(\dot{u}^{n+1})}_l - \frac{\varepsilon^2}{\alpha}Q_l(-\tau)G\widetilde{(u^{n+1}, u^n)}_l,\end{aligned} \tag{3.8}$$

where $G\widetilde{(u^{n+1}, u^n)}_l = G\widetilde{(u^n, u^{n+1})}_l$ clearly holds. The above formula (3.8) can be expressed as

$$\begin{pmatrix}\widetilde{(u^n)}_l + \dfrac{\varepsilon^2}{\alpha}P_l(-\tau)G\widetilde{(u^{n+1}, u^n)}_l\\ \widetilde{(\dot{u}^n)}_l + \dfrac{\varepsilon^2}{\alpha}Q_l(-\tau)G\widetilde{(u^{n+1}, u^n)}_l\end{pmatrix} = \begin{pmatrix}A_l(-\tau) & B_l(-\tau)\\ C_l(-\tau) & D_l(-\tau)\end{pmatrix}\begin{pmatrix}\widetilde{(u^{n+1})}_l\\ \widetilde{(\dot{u}^{n+1})}_l\end{pmatrix}. \tag{3.9}$$

From (3.9) and Lemma 3.1, we obtain

$$\begin{pmatrix}\widetilde{(u^{n+1})}_l\\ \widetilde{(\dot{u}^{n+1})}_l\end{pmatrix} = \begin{pmatrix}A_l(\tau) & B_l(\tau)\\ C_l(\tau) & D_l(\tau)\end{pmatrix}\begin{pmatrix}\widetilde{(u^n)}_l + \dfrac{\varepsilon^2}{\alpha}P_l(-\tau)G\widetilde{(u^{n+1}, u^n)}_l\\ \widetilde{(\dot{u}^n)}_l + \dfrac{\varepsilon^2}{\alpha}Q_l(-\tau)G\widetilde{(u^{n+1}, u^n)}_l\end{pmatrix}. \tag{3.10}$$

From (3.10) and the following relations:

$$\begin{aligned}A_l(\tau)P_l(-\tau) + B_l(\tau)Q_1(-\tau) + P_l(\tau) = 0,\\ C_l(\tau)P_l(-\tau) + D_l(\tau)Q_1(-\tau) + Q_l(\tau) = 0,\end{aligned}$$

we obtain (2.19) and (2.20), which implies that the method SEPEWIFP method is time symmetric. Theorem is proved. □

To prove the existence and uniqueness of the solution for the SEPEWIFP method, we introduce the $M \times M$ matrix T with

$$T_{j,k} = \frac{1}{\sqrt{M}}\mathrm{e}^{\frac{-2ijk\pi}{M}}.$$

It is easy to prove that the matrix T is invertible and satisfies $T^* = T^{-1}$,

Lemma 3.3 (Unique Solvability of SEPEWIFP). *Given u^n and $\dot{u}^n$ $(n \geq 0)$, there exists the solutions u^{n+1} and $\dot{u}^{n+1}$ satisfying the SEPEWIFP method if $\tau \neq 2q\alpha\pi$ for arbitrary integer q. In addition, for sufficiently small values $\tau_0 > 0$ sufficiently small, when $0 < \tau \leq \tau_0$, the solution is unique.*

Proof. Due to $u_0^{n+1} = u_M^{n+1}$ and $\dot{u}_0^{n+1} = \dot{u}_M^{n+1}$, we only analyze the solution

$$\begin{aligned}u^{n+1} &= \left(u_0^{n+1}, \cdots, u_{M-1}^{n+1}\right)^T \in X_M^-,\\ \dot{u}^{n+1} &= \left(\dot{u}_0^{n+1}, \cdots, \dot{u}_{M-1}^{n+1}\right)^T \in X_M^-,\end{aligned}$$

where

$$X_M^- := \mathrm{span}\{v = (v_0, \cdots, v_{M-1})\} \in \mathbb{C}^M.$$

Using

$$u_j^{n+1}=\sum_{l=0}^{M-1}\widetilde{(u^{n+1})}_l \mathrm{e}^{\frac{2ijl\pi}{M}},$$

we express (2.19) as

$$Tu^{n+1}=ATu^n+BT\dot{u}^n-\frac{\varepsilon^2}{\alpha}PTG(u^{n+1},u^n), \tag{3.11}$$

where $A=\operatorname{diag}(A_l(\tau)), B=\operatorname{diag}(B_l(\tau))$ and $P=\operatorname{diag}(P_l(\tau))$ with $l=0,\dots,M-1$. Taking the symbol $u^{n+1/2}=(u^{n+1}+u^n)/2$, we express (3.11) as

$$\begin{aligned}Tu^{n+\frac12}=&\frac12(I_M+A)Tu^n+\frac12 BT\dot{u}^n\\&-\frac{\varepsilon^2}{4\alpha}PT\left(DF\big(2u^{n+\frac12}-u^n\big)+DF(u^n)\right)u^{n+\frac12},\end{aligned} \tag{3.12}$$

where I_M is the $M\times M$ identity matrix and

$$DF(w)=\operatorname{diag}\left(|w_0|^2,|w_1|^2,\cdots,|w_{M-1}|^2\right),\quad w\in X_M^-.$$

From Lemma 3.2, when $\tau\neq 2q\alpha\pi$ for arbitrary integer q, we have $\mathrm{Re}P_l^{-1}(\tau)>0$. So the matrix P is invertible. Multiplying both sides of (3.12) from left by T^*P^{-1}, we obtain

$$\begin{aligned}T^*P^{-1}Tu^{n+\frac12}=&\frac12T^*P^{-1}(I_M+A)Tu^n+\frac12T^*P^{-1}BT\dot{u}^n\\&-\frac{\varepsilon^2}{4\alpha}\left(DF\big(2u^{n+\frac12}-u^n\big)+DF(u^n)\right)u^{n+\frac12}.\end{aligned}$$

Define a continuous map $\mathcal{F}^n: X_M^-\to X_M^-$ as

$$\begin{aligned}\mathcal{F}^nw=&T^*P^{-1}Tw-\frac12T^*P^{-1}(I_M+A)Tu^n-\frac12T^*P^{-1}BT\dot{u}^n\\&+\frac{\varepsilon^2}{4\alpha}\big(DF(2w-u^n)+DF(u^n)\big)w.\end{aligned}$$

Introducing the inner product $\langle u,v\rangle=h\sum_{j=0}^{M-1}\bar{u}_jv_j$ and the norm $\|u\|_{l^2}=\sqrt{\langle u,u\rangle}$, it is easy to get

$$\begin{aligned}\mathrm{Re}\,\langle T^*P^{-1}Tw,w\rangle&=\mathrm{Re}\,\langle P^{-1}Tw,Tw\rangle\\&=\frac12\left(\langle P^{-1}Tw,Tw\rangle+\langle Tw,P^{-1}Tw\rangle\right)\\&=\frac12\left(\langle P^{-1}Tw,Tw\rangle+\langle (P^{-1})^*Tw,Tw\rangle\right)\\&=\langle \mathrm{Re}\,P^{-1}Tw,Tw\rangle,\end{aligned}$$

where $\mathrm{Re}P^{-1}=\operatorname{diag}(\mathrm{Re}P_l^{-1}(\tau))$ is a positive definite matrix. For a matrix, we use $\|\cdot\|$ to denote its spectral norm. The fact

$$\begin{aligned}\mathrm{Re}\langle\mathcal{F}^nw,w\rangle=&\mathrm{Re}\langle T^*P^{-1}Tw,w\rangle-\frac12\mathrm{Re}\left\langle T^*P^{-1}(I_M+A)Tu^n+T^*P^{-1}BT\dot{u}^n,w\right\rangle\\&+\frac{\varepsilon^2}{4\alpha}\mathrm{Re}\left\langle\big(DF(2w-u^n)+DF(u^n)\big)w,w\right\rangle\end{aligned} \tag{3.13}$$

$$
\begin{aligned}
&\geq \langle \mathrm{Re}P^{-1}Tw, Tw\rangle - \frac{1}{2}\mathrm{Re}\left\langle T^*P^{-1}(I_M+A)Tu^n + T^*A_3^{-1}BT\dot{u}^n, w\right\rangle \\
&\geq \left\|(\mathrm{Re}P^{-1})^{\frac{1}{2}}T\right\|^{-2}\|w\|_{l^2}^2 - \frac{1}{2}\mathrm{Re}\left\langle T^*P^{-1}(I_M+A_1)Tu^n + T^*P^{-1}A_2T\dot{u}^n, w\right\rangle \\
&\geq \left\|w\right\|_{l^2}\left(\left\|(\mathrm{Re}P^{-1})^{\frac{1}{2}}T\right\|^{-2}\|w\|_{l^2} - \frac{1}{2}\left\|T^*P^{-1}(I_M+A)Tu^n + T^*P^{-1}BT\dot{u}^n\right\|_{l^2}\right)
\end{aligned}
$$

implies

$$\lim_{\|w\|_{l^2}\to\infty}\frac{\langle \mathcal{F}^n w, w\rangle}{\|w\|_{l^2}} = \infty.$$

From the Brouwer fixed point theorem [4,9], we can conclude that there exists w^* such that $\mathcal{F}^n w^* = 0$, which implies that the Eq. (2.19) is solvable.

Now, we proceed to prove the uniqueness of the numerical solution. Suppose that there are two solutions $u^{n+1}, v^{n+1} \in X_M^-$ to the SEPEWIFP method. From Theorem 4.1 in the next section, we get

$$\|u^n\|_\infty \leq CE^0, \quad \|u^{n+1}\|_\infty \leq CE^0, \quad \|v^{n+1}\|_\infty \leq CE^0. \tag{3.14}$$

Denoting $w^{n+1} = u^{n+1} - v^{n+1} \in X_M^-$, we have from (3.11) that

$$w^{n+1} = -\frac{\varepsilon^2}{\alpha}T^*PT\big(G(u^{n+1}, u^n) - G(v^{n+1}, u^n)\big). \tag{3.15}$$

Using $|P_l(\tau)| \leq \tau^2/2$ in (3.15), we obtain

$$
\begin{aligned}
\|w^{n+1}\|_{l^2} &\leq \frac{\varepsilon^2}{\alpha}\|T^*PT\|\,\|G(u^{n+1}, u^n) - G(v^{n+1}, u^n)\|_{l^2} \\
&= \frac{\varepsilon^2}{4\alpha}\|P\|\,\big\|\big(|u^{n+1}|^2 + |u^n|^2\big)w^{n+1} + \big(|v_{n+1}|^2 - |u_{n+1}|^2\big)(v_{n+1}+u_n)\big\|_{l^2} \\
&\leq \frac{3}{4\alpha}\varepsilon^2\tau^2(E^0)^2\|w^{n+1}\|_{l^2}.
\end{aligned}
$$

Thus, for sufficiently small value τ, we have

$$\|w^{n+1}\|_{l^2} = \|u^{n+1} - v^{n+1}\|_{l^2} = 0 \ \Rightarrow\ u^{n+1} = v^{n+1},$$

i.e. the SEPEWIFP method (2.18)-(2.20) has the unique solution. The existence and uniqueness of solution $\dot{u}^{n+1}$ are obvious because that the formula (2.20) is explicit. □

4. Energy-Preservation

Firstly we introduce the lemma.

Lemma 4.1. *Given $u, v \in X_M$ and $\widetilde{u}_l, \widetilde{v}_l$ defined in* (2.6), *we have*

$$h\sum_{j=0}^{M-1}\overline{u}_j v_j = (b-a)\sum_{l\in\Omega_M}\overline{\widetilde{u}}_l\widetilde{v}_l. \tag{4.1}$$

From this lemma, we obtain the following results about the discrete energy.

Theorem 4.1. *The SEPEWIFP method preserves exactly the energy in discrete level as*

$$E^n := \alpha\|\dot{u}^n\|_{l^2}^2 + \big\|D_x u^n\big\|_{l^2}^2 + \varepsilon^2 h \sum_{j=0}^{M-1} F\big(|u_j^n|^2\big)$$
$$\equiv \alpha\|\dot{u}^0\|_{l^2}^2 + \big\|D_x u^0\big\|_{l^2}^2 + \varepsilon^2 h \sum_{j=0}^{M-1} F\big(|u_j^0|^2\big) =: E^0, \quad n = 0, 1, \ldots. \tag{4.2}$$

Here

$$\|u\|_{l^2}^2 = h \sum_{j=0}^{M-1} |u_j|^2, \quad F(v) = \frac{1}{2}v^2,$$

and

$$\big(D_x u^n\big)_j = \sum_{l\in\Omega_M} i\mu_l \widetilde{(u^n)}_l e^{i\mu(x_j-a)} = \sum_{l\in\Omega_M} i\mu_l \widetilde{(u^n)}_l e^{\frac{2ijl\pi}{M}}. \tag{4.3}$$

Proof. Based on Lemma 4.1, the discrete energy (4.2) can be expressed as

$$E^n := \sum_{l\in\Omega_M} (b-a)\left[\alpha\big|\widetilde{(\dot{u}^n)}_l\big|^2 + \mu_l^2\big|\widetilde{(u^n)}_l\big|^2\right] + \varepsilon^2 h \sum_{j=0}^{M-1} F\big(|u_j^n|^2\big), \quad n = 0, 1, \ldots. \tag{4.4}$$

Inserting (2.19) and (2.20) into (4.4), we have

$$\begin{aligned}\frac{E^{n+1}-E^n}{b-a} :=& \sum_{l\in\Omega_M} \alpha\left|C_l(\tau)\widetilde{(u^n)}_l + D_l(\tau)\widetilde{(\dot{u}^n)}_l - Q_1(\tau)\widetilde{S_l^n}\right|^2\\ &+ \sum_{l\in\Omega_M} \mu_l^2\left|A_l(\tau)\widetilde{(u^n)}_l + B_l(\tau)\widetilde{(\dot{u}^n)}_l - P_1(\tau)\widetilde{S_l^n}\right|^2\\ &- \sum_{l\in\Omega_M} \alpha\big|\widetilde{(\dot{u}^n)}_l\big|^2 - \sum_{l\in\Omega_M} \mu_l^2\big|\widetilde{(u^n)}_l\big|^2\\ &+ \frac{\varepsilon^2 h}{b-a}\sum_{j=0}^{M-1}\Big(F\big(|u_j^{n+1}|^2\big) - F\big(|u_j^n|^2\big)\Big),\end{aligned} \tag{4.5}$$

where

$$S_l^n = \frac{\varepsilon^2}{\alpha} G(u^{n+1}, u^n). \tag{4.6}$$

On the other hand, it holds that

$$\begin{aligned}&2(b-a)\mathrm{Re}\sum_{l\in\Omega_M} \overline{\widetilde{S_l^n}}\big(\widetilde{(u^{n+1})}_l - \widetilde{(u^n)}_l\big)\\ =& 2\frac{\varepsilon^2 h}{\alpha}\mathrm{Re}\sum_{j=0}^{M-1} \overline{G(u^{n+1},u^n)_j}\big(u_j^{n+1} - u_j^n\big)\\ =& \frac{\varepsilon^2 h}{2\alpha}\mathrm{Re}\sum_{j=0}^{M-1} \big(|u_j^{n+1}|^2 + |u_j^n|^2\big)\overline{\big(u_j^{n+1} + u_j^n\big)}\big(u_j^{n+1} - u_j^n\big)\\ =& \frac{\varepsilon^2 h}{2\alpha}\sum_{j=0}^{M-1} \big(|u_j^{n+1}|^2 + |u_j^n|^2\big)\big(|u_j^{n+1}|^2 - |u_j^n|^2\big)\\ =& \frac{\varepsilon^2}{\alpha} h\sum_{j=0}^{M-1} \Big[F\big(|u_j^{n+1}|^2\big) - F\big(|u_j^n|^2\big)\Big].\end{aligned} \tag{4.7}$$

From the following relations:

$$\begin{aligned}
&\alpha\overline{C_l}(\tau)D_l(\tau)+\mu_l^2\mathrm{Re}(\overline{A_l}(\tau)B_l(\tau)=0,\\
&\frac{\mu_l^2}{\alpha}|A_l(\tau)|^2+|C_l(\tau)|^2=\frac{\mu_l^2}{\alpha},\\
&\frac{\mu^2}{\alpha}|B_l(\tau)|^2+|D_l(\tau)|^2=1,
\end{aligned}\tag{4.8}$$

and inserting (4.7) into (4.5), we have

$$\begin{aligned}
\frac{E^{n+1}-E^n}{b-a}:=&-\sum_{l\in\Omega_M}2\mathrm{Re}\left(\alpha C_l(\tau)\overline{Q_l}(\tau)+\mu_l^2A_l(\tau)\overline{P_l}(\tau)\right)\widetilde{(u^n)}_l\overline{\widetilde{(S^n)}_l}\\
&-\sum_{l\in\Omega_M}2\mathrm{Re}\left(\alpha D_l(\tau)\overline{Q_l}(\tau)+\mu_l^2B_1(\tau)\overline{P_l}(\tau)\right)\widetilde{(\dot{u}^n)}_l\overline{\widetilde{(S^n)}_l}\\
&+\sum_{l\in\Omega_M}\left(\alpha|Q_l(\tau)|^2+\mu_l^2|P_l(\tau)|^2\right)\left|\widetilde{S_l^n}\right|^2\\
&+2\alpha\mathrm{Re}\sum_{l\in\Omega_M}\left(\widetilde{(u^{n+1})}_l-\widetilde{(u^n)}_l\right)\overline{\widetilde{(S^n)}_l}.
\end{aligned}\tag{4.9}$$

Inserting (2.19) into (4.9), we have

$$\begin{aligned}
\frac{E^{n+1}-E^n}{b-a}:=&-\sum_{l\in\Omega_M}2\mathrm{Re}\left[\left(\alpha C_l(\tau)\overline{Q_l}(\tau)+\mu_l^2A_l(\tau)\overline{P_l}(\tau)-\alpha A_l(\tau)+\alpha\right)\widetilde{(u^n)}_l\overline{\widetilde{(S^n)}_l}\right]\\
&-\sum_{l\in\Omega_M}2\mathrm{Re}\left[\left(\alpha D_l(\tau)\overline{Q_l}(\tau)+\mu_l^2B_1(\tau)\overline{P_l}(\tau)-\alpha B_1(\tau)\right)\widetilde{(\dot{u}^n)}_l\overline{\widetilde{(S^n)}_l}\right]\\
&+\sum_{l\in\Omega_M}\left(\alpha|Q_l(\tau)|^2+\mu_l^2|P_l(\tau)|^2-2\alpha\mathrm{Re}P_l(\tau)\right)\left|\widetilde{(S^n)}_l\right|^2.
\end{aligned}\tag{4.10}$$

It is easy to verify that the following relationship holds:

$$\begin{aligned}
&\alpha C_l(\tau)\overline{Q_l}(\tau)+\mu_l^2A_l(\tau)\overline{P_l}(\tau)-\alpha A_l(\tau)+\alpha=0,\\
&\alpha D_l(\tau)\overline{Q_l}(\tau)+\mu_l^2B_1(\tau)\overline{P_l}(\tau)-\alpha B_1(\tau)=0,\\
&\alpha|Q_l(\tau)|^2+\mu_l^2|P_l(\tau)|^2-2\alpha\mathrm{Re}P_l(\tau)=0.
\end{aligned}\tag{4.11}$$

Plugging (4.11) into (4.10) results in $E^{n+1}\equiv E^n$ for $n=0,1,\ldots$, which implies that the result (4.2) holds. □

For the projection and interpolation errors, we have lemma.

Lemma 4.2 ([36]). *For any $\mu,k\geq 0$, we obtain*

$$\|u-P_M(u)\|_\mu\leq Ch^k\|u\|_{\mu+k},\quad \|P_M(u)\|_{\mu+k}\leq C\|u\|_{\mu+k},\quad u\in H_p^{\mu+k}(\Omega).\tag{4.12}$$

Moreover, if $\mu+k>1/2$, we have

$$\|u-I_M(u)\|_\mu\leq Ch^k\|u\|_{\mu+k},\quad \|I_M(u)\|_{\mu+k}\leq C\|u\|_{\mu+k},\quad u\in H_p^{\mu+k}(\Omega).\tag{4.13}$$

Here the generic constant $C>0$ does not depend on h and f.

Lemma 4.3. *For $\mu > 1/2, u_1, u_2, w \in H^\mu(\Omega)$, we obtain*

$$\left\| \left(|u_1|^2 - |u_2|^2\right) w \right\|_\mu \leq (\|u_1\|_\mu + \|u_2\|_\mu)\|u_1 - u_2\|_\mu \|w\|_\mu. \tag{4.14}$$

Proof. It is easy to get

$$\left(|u_1|^2 - |u_2|^2\right) w = \mathrm{Re}\overline{(u_1 + u_2)}(u_1 - u_2)w.$$

Then the bilinear estimate

$$\|fg\|_\mu \leq C_\mu \|f\|_\mu \|g\|_\mu, \quad f, g \in H^\mu(\Omega), \quad \mu > 1/2, \tag{4.15}$$

immediately confirms the correctness of the conclusion. □

Lemma 4.4. *For $k > 1/2$ and sufficiently regular u, w, we have*

$$\begin{aligned} &\left\| |u_1|^2 u_2 \right\|_k \leq \|u_1\|_k^2 \|u_2\|_k, \\ &\left\| \partial_t |u_1|^2 u_2 \right\|_k \leq 2\|u_1\|_k \|\partial_t u_1\|_k \|u_2\|_k, \\ &\left\| \partial_{tt} |u_1|^2 u_2 \right\|_k \leq 2\left(\|\partial_t u_1\|_k^2 + \|u_1\|_k \|\partial_{tt} u_1\|_k\right)\|u_2\|_k. \end{aligned} \tag{4.16}$$

Lemma 4.5. *For the functions given in (2.13) and (2.14), we have*

$$A_l'(s) = C_l(s), \quad B_l'(s) = D_l(s), \quad P_l'(s) = Q_l(s).$$

Lemma 4.6. *For the functions given in (2.13) and (2.14), we have the following bounds:*

$$\begin{aligned} &|A_l(s)| \leq 1, \quad |B_l(s)| \leq |s|, \qquad |C_l(s)| \leq \frac{\mu_l^2}{\alpha}|s|, \\ &|D_l(s)| \leq 1, \quad |P_l(s)| \leq 2\alpha|s|, \quad |Q_l(s)| \leq |s|, \\ &\left| \int_0^s B_l(s-z) z \mathrm{d}z - \frac{s}{2} P_l(s) \right| \leq \frac{s^3}{12}, \quad \left| \int_0^s D_l(s-z) z \mathrm{d}z - \frac{s}{2} Q_l(s) \right| \leq \frac{s^3}{12\alpha}. \end{aligned}$$

Proof. The first four results and the sixth result are obvious. Due to $|B_l(s)| \leq 2|\alpha|$, we obtain the fifth result. To prove the seventh inequality, we denote

$$\int_0^s B_l(s-z) z \mathrm{d}z - \frac{s}{2} P_l(s) = \int_0^s B_l(s-z) \left(z - \frac{s}{2}\right) \mathrm{d}z.$$

Using the Taylor expansion based on the integral remainder, we obtain

$$\begin{aligned} &\int_0^s B_l(s-z) z \mathrm{d}z - \frac{s}{2} P_l(s) \\ &= \int_0^s B_l(s-z) \mathrm{d}\left(\frac{z^2}{2} - \frac{sz}{2}\right) \\ &= \left[B_l(s-z)\left(\frac{z^2}{2} - \frac{sz}{2}\right)\right]_0^s - \int_0^s \left(\frac{z^2}{2} - \frac{sz}{2}\right)\left[\frac{\mathrm{d}}{\mathrm{d}z} B_l(s-z)\right] \mathrm{d}z \\ &= \int_0^s \left(\frac{z^2}{2} - \frac{sz}{2}\right) B_l'(s-z) \mathrm{d}z. \end{aligned} \tag{4.17}$$

From $B_l'(s) = D_l(s)$ in Lemma 4.5, we have

$$\begin{aligned} \left| \int_0^s B_l(s-z) z \mathrm{d}z - \frac{s}{2} P_l(s) \right| &\leq \int_0^s \left| \frac{z^2}{2} - \frac{sz}{2} \right| \left| B_l'(s-z) \right| \mathrm{d}z \\ &\leq \frac{1}{2} \int_0^s z(s-z) \mathrm{d}z \leq \frac{s^2}{12}, \end{aligned} \tag{4.18}$$

and we are done. Similarly, we can prove the last result. □

5. Convergence Result

For our convergence analysis, we assume that the true solution of (2.1) in the time interval $[0, T_0/\varepsilon^\beta]$ satisfies

$$u \in C\left([0, T_0/\varepsilon^\beta]; H_p^{m_0+m}\right) \cap C^1\left([0, T_0/\varepsilon^\beta]; H_p^{m+m_0-1}\right) \cap C^2\left([0, T_0/\varepsilon^\beta]; H_p^m\right), \tag{A}$$

where $m_0 \geq 2, m > 1/2$ and

$$H_p^m(\Omega) = \left\{u \in H^m(\Omega),\, \partial_x^l(a) = \partial_x^l(b),\, 0 \leq l \leq m-1\right\}.$$

Define the norm in $H_p^m(\Omega)$ as

$$\|f\|_{m,p}^2 = \sum_{l \in Z} |\mu_l|^{2m} |\hat{f}_l|^2, \quad f(x) = \sum_{l \in Z} \hat{f}_l e^{i\mu_l(x-a)}, \quad \mu_l = \frac{2\pi l}{b-a}, \tag{5.1}$$

which is equivalent to the H^m norm (2.3) in $H_p^m(\Omega)$. In this paper, we still refer to the norm (5.1) as $\|\cdot\|_m$. That is, in our error analysis, we always use the notation $\|\cdot\|_m$ for the norm (5.1). Define the error function as

$$e^n := u(x, t_n) - I_M u^n, \quad \dot{e}^n := \partial_t u(x, t_n) - I_M \dot{u}^n, \quad n = 0, 1, \ldots, T_0\varepsilon^{-\beta}/\tau \tag{5.2}$$

with $u^n, \dot{u}^n \in X_M$ being the approximations provided by the SEPEWIFP method. Then we obtain the error analysis results of the SEPEWIFP method as follows.

Theorem 5.1. *Under the assumption* (A)*, there exist sufficiently small constants $h_0 > 0$ and $\tau_0 > 0$, which are independent of ε and satisfy the conditions of Lemma* 3.3*, such that for any $0 < \varepsilon \leq 1$, when $0 < h \leq h_0$ and $0 < \tau \leq \varepsilon^{\beta/2-1}\tau_0$, we obtain the error bounds for $0 \leq n \leq T_0\varepsilon^{-\beta}/\tau$ as*

$$\begin{aligned} &\|e^n(x)\|_m \lesssim h^{m_0} + \varepsilon^{2-\beta}\tau^2, \qquad \left\|I_M u^n\right\|_m \leq 1 + M_u \\ &\|\dot{e}^n(x)\|_{m-1} \lesssim h^{m_0} + \varepsilon^{2-\beta}\tau^2, \quad \left\|I_M \dot{u}^n\right\|_{m-1} \leq 1 + M_u', \end{aligned} \tag{5.3}$$

where

$$\begin{aligned} M_u &:= \|u(x,t)\|_{L^\infty([0,T_0/\varepsilon^\beta]; H^m(\Omega))} \\ M_u' &:= \|\partial_t u(x,t)\|_{L^\infty([0,T_0/\varepsilon^\beta]; H^{m-1}(\Omega))}. \end{aligned}$$

Remark 5.1. Crank-Nicolson finite-difference (CNFD) methods have been proposed for the NLSW (1.1) with $\varepsilon = 1$ and proved to be energy-preserving [14, 15, 23, 28, 38]. In the weak nonlinear case $0 < \varepsilon \ll 1$, we can take a very similar analysis which has been taken for the long-time dynamics of the KG equations and Dirac equations with weak nonlinearity or small potential [8, 18, 22] and conclude that under the sufficient regularity conditions, the errors of CNFD methods are $\mathcal{O}(\varepsilon^{-\beta}h^2 + \varepsilon^{-\beta}\tau^2)$ up to the time at $\mathcal{O}(1/\varepsilon^\beta)$ with $\beta \in [0, 2]$. That means that for CNFD, in order to obtain a reasonable numerical solution, we must take very small time step $\tau = \mathcal{O}(\varepsilon^{\beta/2})$ and mesh size $h = \mathcal{O}(\varepsilon^{\beta/2})$, respectively. This is an unsatisfactory result because the limit on the time step τ and mesh size h is too strict. In contrast, our SEPEWIFP method not only preserve the energy but also is uniformly bounded with respect to h and τ in the long-term integration interval $[0, T_0/\varepsilon^\beta]$ with $\beta \in [0, 2]$. More specifically, for SEPEWIFP method, in order to obtain a reasonable numerical solution, we just take the time step $\tau = \mathcal{O}(\varepsilon^{\beta/2-1})$ and mesh size $h = \mathcal{O}(1)$, respectively, which allow for larger scales in time step.

The main difficulty in proving Theorem 5.1 is to show that $\|I_M u^n\|_m \lesssim 1$. For this goal, we adapt the cut-off technique [5, 29]. Denote $B = 1 + M_u$ and define

$$|u|_B^2 = \rho\left(\|u\|_m/B\right)|u|^2 \quad \text{with} \quad \rho(\theta) = \begin{cases} 1, & 0 \le \theta \le 1, \\ \in [0,1], & 1 \le \theta \le 2, \\ 0, & \theta \ge 2, \end{cases} \tag{5.4}$$

where $\rho(\theta) \in C_0^\infty(\mathbb{R}^+)$. For the function $|u|_B^2$, we have lemma.

Lemma 5.1. *Given $m > 1/2$, for $w \in H^m(\Omega), u_1, u_2$ and $|u|_B^2$ defined in* (5.4)*, the following inequality holds:*

$$\left\|\left(|u_1|_B^2 - |u_2|_B^2\right)w\right\|_m \le C_B\|u_1 - u_2\|_m\|w\|_m, \quad w \in H^m(\Omega), \tag{5.5}$$

where $C_B = 4B(1 + \max_{\theta\in[0,2]}|\rho'(\theta)|)$ with $B = 1 + M_u$.

Proof. The proof is similar to that of [17, Lemma 3.1] and is omitted here. We should note that here u_1 and u_2 are complex valued functions. □

We introduce the following modified EWIFP (MEWIFP) method by choosing $\bar{u}_j^0 = u_j^0$, $\dot{\bar{u}}_j^0 = \dot{u}_j^0$ and for $n = 0, 1, \ldots,$

$$\bar{u}_j^{n+1} = \sum_{l\in\Omega_M} \widetilde{(\bar{u}^{n+1})}_l e^{\frac{2ijl\pi}{M}}, \quad \dot{\bar{u}}_j^{n+1} = \sum_{l\in\Omega_M} \widetilde{(\dot{\bar{u}}^{n+1})}_l e^{\frac{2ijl\pi}{M}}, \tag{5.6}$$

where

$$\widetilde{(\bar{u}^{n+1})}_l = A_l(\tau)\widetilde{(\bar{u}^n)}_l + B_l(\tau)\widetilde{(\dot{\bar{u}}^n)}_l - \frac{\varepsilon^2}{\alpha}P_l(\tau)\widetilde{G_B\left(I_M\bar{u}^{n+1}, I_M\bar{u}^n\right)}_l, \tag{5.7}$$

$$\widetilde{(\dot{\bar{u}}^{n+1})}_l = C_l(\tau)\widetilde{(\bar{u}^n)}_l + D_l(\tau)\widetilde{(\dot{\bar{u}}^n)}_l - \frac{\varepsilon^2}{\alpha}Q_l(\tau)\widetilde{G_B\left(I_M\bar{u}^{n+1}, I_M\bar{u}^n\right)}_l \tag{5.8}$$

with $G_B(u, v)$ given by

$$G_B(u, v) = \frac{1}{4}\left(|u|_B^2 + |v|_B^2\right)(u + v). \tag{5.9}$$

Define the error function as

$$\bar{e}^n := u(x, t_n) - I_M\bar{u}^n, \quad \dot{\bar{e}}^n := \partial_t u(x, t_n) - I_M\dot{\bar{u}}^n, \quad n = 0, 1, \ldots, T_0\varepsilon^{-\beta}/\tau. \tag{5.10}$$

Lemma 5.2. *Based on the assumption* (A)*, we have for $G_B(u, v)$ of* (5.9)*,*

$$\begin{aligned} &\left\|G_B\left(u(x, t_{n+1}), u(x, t_n)\right)\right\|_{m+m_0} \le \|u(x, t)\|^3_{L^\infty([0,T/\varepsilon^\beta];H^{m+m_0}(\Omega))}, \\ &\left\|G_B\left(u(x, t_{n+1}), u(x, t_n)\right) - G_B\left(I_M\bar{u}^{n+1}, I_M\bar{u}^n\right)\right\|_m \le C_{B2}\left(\|\bar{e}^{n+1}\|_m + \|\bar{e}^n\|_m\right), \end{aligned} \tag{5.11}$$

where $C_{B2} = (C_B M_u + 2B^2)/2$ with $C_B = 4B(1 + \max_{\theta\in[0,2]}|\rho'(\theta)|)$.

Proof. The proof is similar to that of [17, Lemma 3.1] but here $u(x, t_{n+1}), u(x, t_n), I_M\bar{u}^{n+1}$ and $I_M\bar{u}^n$ are complex valued functions.

With $\bar{u}^n, \dot{\bar{u}}^n \in X_M$ being the approximations provided by the MEWIFP method, we obtain error analysis results of the MEWIFP method as follows.

Theorem 5.2. *Under the assumption* (A)*, there exist sufficiently small constants* $h_0 > 0$ *and* $\tau_0 > 0$*, which are independent of* ε *and satisfy the conditions of Lemma* 3.3*, such that for any* $0 < \varepsilon \leq 1$*, when* $0 < h \leq h_0$ *and* $0 < \tau \leq \varepsilon^{\beta/2-1}\tau_0$*, we obtain the error bounds for* $0 \leq n \leq T_0\varepsilon^{-\beta}/\tau$ *as*

$$\|\bar{e}^n(x)\|_m \lesssim h^{m_0} + \varepsilon^{2-\beta}\tau^2, \qquad \left\|I_M\bar{u}^n\right\|_m \leq 1 + M_u, \tag{5.12}$$

$$\|\bar{\dot{e}}^n(x)\|_{m-1} \lesssim h^{m_0} + \varepsilon^{2-\beta}\tau^2, \quad \left\|I_M\bar{\dot{u}}^n\right\|_{m-1} \leq 1 + M'_u, \tag{5.13}$$

where

$$M_u := \|u(x,t)\|_{L^\infty([0,T_0/\varepsilon^\beta];H^m(\Omega))},$$
$$M'_u := \|\partial_t u(x,t)\|_{L^\infty([0,T_0/\varepsilon^\beta];H^{m-1}(\Omega))}.$$

Proof. Firstly, we introduce the projected error $\bar{e}^n_M(x)$ and $\bar{\dot{e}}^n_M(x)$ as

$$\bar{e}^n_M(x) = P_M u(x,t_n) - I_M\bar{u}^n(x), \quad \bar{\dot{e}}^n_M(x) = P_M\partial_t u(x,t_n) - I_M\bar{\dot{u}}^n(x). \tag{5.14}$$

Using triangle inequality and Lemma 4.2 and taking into account the assumption (A), we have

$$\begin{aligned}
\|\bar{e}^n(x)\|_m &\leq \left\|\bar{e}^n_M\right\|_m + \|u(x,t_n) - P_M u(x,t_n)\|_m \\
&\leq \left\|\bar{e}^n_M\right\|_m + Ch^{m_0}\|u(t_n,x)\|_{m+m_0} \lesssim \left\|\bar{e}^n_M\right\|_m + h^{m_0}, \\
\|\bar{\dot{e}}^n(x)\|_{m-1} &\leq \left\|\bar{\dot{e}}^n_M\right\|_{m-1} + \|\partial_t u(x,t_n) - P_M\partial_t u(x,t_n)\|_{m-1} \\
&\leq \left\|\bar{\dot{e}}^n_M\right\|_{m-1} + Ch^{m_0}\|\partial_t u(t_n,x)\|_{m+m_0-1} \lesssim \left\|\bar{\dot{e}}^n_M\right\|_{m-1} + h^{m_0}.
\end{aligned} \tag{5.15}$$

Obviously, we can transform the proof of (5.12)-(5.13) to the estimates for $\bar{e}^n_M$ and $\bar{\dot{e}}^n_M$, which often require the following three steps.

Step 1. Bounds of local truncation errors. Plugging Fourier series

$$u(x,t) = \sum_{l\in Z}\widehat{u}_l(t)\mathrm{e}^{i\mu_l(x-a)}$$

for the true solution of (2.1) into (5.7) and (5.8), we obtain

$$\begin{aligned}
\widehat{u}_l(t_{n+1}) &= A_l(\tau)\widehat{u}_l(t_n) + B_l(\tau)\widehat{\dot{u}}_l(t_n) - \frac{\varepsilon^2}{\alpha}P_l(\tau)G_B\big(u(x,\widehat{t_{n+1}),u(x},t_n)\big)_l + \widehat{\bar{\xi}_l^{n+1}}, \\
\widehat{\dot{u}}_l(t_{n+1}) &= C_l(\tau)\widehat{u}_l(t_n) + D_l(\tau)\widehat{\dot{u}}_l(t_n) - \frac{\varepsilon^2}{\alpha}Q_l(\tau)G_B\big(u(x,\widehat{t_{n+1}),u(x},t_n)\big)_l + \widehat{\bar{\dot{\xi}}_l^{n+1}}.
\end{aligned} \tag{5.16}$$

The Fourier coefficients of $u(x,t)$ satisfy

$$\frac{\mathrm{d}^2}{\mathrm{d}t^2}\widehat{u}_l(t) = \frac{i}{\alpha}\frac{\mathrm{d}}{\mathrm{d}t}\widehat{u}_l(t) - \frac{|\mu_l|^2}{\alpha}\widehat{u}_l(t) - \frac{\varepsilon^2}{\alpha}\widehat{G(u)}_l(t), \quad l\in\Omega_M, \quad t\geq 0. \tag{5.17}$$

From (5.17), we have

$$\begin{aligned}
\widehat{u}_l(t_{n+1}) &= A_l(\tau)\widehat{u}_l(t_n) + B_l(\tau)\widehat{\dot{u}}_l(t_n) - \frac{\varepsilon^2}{\alpha}\int_0^\tau B_l(\tau-z)\widehat{G(u)}_l(t_n+z)\mathrm{d}z, \\
\widehat{\dot{u}}_l(t_{n+1}) &= C_l(\tau)\widehat{u}_l(t_n) + D_l(\tau)\widehat{\dot{u}}_l(t_n) - \frac{\varepsilon^2}{\alpha}\int_0^\tau D_l(\tau-z)\widehat{G(u)}_l(t_n+z)\mathrm{d}z.
\end{aligned} \tag{5.18}$$

Subtract (5.16) from the above formula, we get

$$\begin{aligned}
\widehat{\bar{\xi}_l^{n+1}} &= -\frac{\varepsilon^2}{\alpha}\left(\int_0^\tau B_l(\tau-z)\widehat{G(u)}_l(t_n+z)\mathrm{d}z - P_l(\tau)G_B\big(u(x,\widehat{t_{n+1}),u(x},t_n)\big)_l\right),\\
\widehat{\dot{\bar{\xi}}_l^{n+1}} &= -\frac{\varepsilon^2}{\alpha}\left(\int_0^\tau D_l(\tau-z)\widehat{G(u)}_l(t_n+z)\mathrm{d}z - Q_l(\tau)G_B\big(u(x,\widehat{t_{n+1}),u(x},t_n)\big)_l\right).
\end{aligned} \tag{5.19}$$

From the definition (5.9), we obtain

$$G_B\big(u(x,t_{n+1}),u(x,t_n)\big) = G\big(u(x,t_{n+1}),u(x,t_n)\big),$$

respectively with

$$\begin{aligned}
\widehat{\bar{\xi}_l^{n+1}} &= -\frac{\varepsilon^2}{\alpha}\left(\int_0^\tau B_l(\tau-z)\widehat{G(u)}_l(t_n+z)\mathrm{d}z - P_l(\tau)G\big(u(x,\widehat{t_{n+1}),u(x},t_n)\big)_l\right),\\
\widehat{\bar{\dot{\xi}}_l^{n+1}} &= -\frac{\varepsilon^2}{\alpha}\left(\int_0^\tau D_l(\tau-z)\widehat{G(u)}_l(t_n+z)\mathrm{d}z - Q_l(\tau)G\big(u(x,\widehat{t_{n+1}),u(x},t_n)\big)_l\right).
\end{aligned} \tag{5.20}$$

For the convenience of expression, we denote

$$(Gu)(x,t) = G\big(u(x,t)\big) = |u(x,t)|^2 u(x,t). \tag{5.21}$$

Using Taylor's expansion, we obtain

$$(Gu)(x,t_n+z) = (Gu)\big(x,t_{n+\frac12}\big) + \left(z-\frac{\tau}{2}\right)\partial_t(Gu)(x,t_n) + R_1(x,t_n,z), \tag{5.22}$$

where $t_{n+1/2} = t_n + \tau/2$ and the integral remainder is

$$R_1(x,t_n,z) = \left(z-\frac{\tau}{2}\right)^2 \int_0^1 (1-\xi)\partial_{tt}(Gu)\left(x, t_{n+\frac12} + \xi\left(z-\frac{\tau}{2}\right)\right)\mathrm{d}\xi. \tag{5.23}$$

On the other hand, using Taylor's expansion, we have

$$\begin{aligned}
G\big(u(x,t_{n+1}),u(x,t_n)\big) &= \frac14\big(|u(x,t_{n+1})|^2 + |u(x,t_n)|^2\big)\big(u(x,t_{n+1})+u(x,t_n)\big)\\
&= \left(\big|u\big(x,t_{n+\frac12}\big)\big|^2 + \frac12\int_{-\tau/2}^{\tau/2}\left(\frac{\tau}{2}-|z|\right)\partial_{tt}\big|u\big(x,t_{n+\frac12}+z\big)\big|^2\mathrm{d}z\right)\\
&\quad\times\left(u\big(x,t_{n+\frac12}\big) + \frac12\int_{-\tau/2}^{\tau/2}\left(\frac{\tau}{2}-|z|\right)\partial_{tt}u\big(x,t_{n+\frac12}+z\big)\mathrm{d}z\right)\\
&= \big|u\big(x,t_{n+\frac12}\big)\big|^2 u\big(x,t_{n+\frac12}\big) + R_2(x,t_n),
\end{aligned} \tag{5.24}$$

where

$$\begin{aligned}
R_2(x,t_n) = &\frac12\big|u\big(x,t_{n+\frac12}\big)\big|^2\int_{-\tau/2}^{\tau/2}\left(\frac{\tau}{2}-|z|\right)\partial_{tt}u\big(x,t_{n+\frac12}+z\big)\mathrm{d}z\\
&+\frac14\int_{-\tau/2}^{\tau/2}\left(\frac{\tau}{2}-|z|\right)\partial_{tt}\big|u\big(x,t_{n+\frac12}+z\big)\big|^2\mathrm{d}z\big(u(x,t_{n+1})+u(x,t_n)\big).
\end{aligned} \tag{5.25}$$

Plugging (5.22) and (5.24) into (5.20), respectively, and using (2.13), we obtain

$$\begin{aligned}\widehat{\bar{\xi}_l^{n+1}} &= -\frac{\varepsilon^2}{\alpha}\left(\int_0^\tau B_l(\tau-z)z\mathrm{d}z - \frac{\tau}{2}P_l(\tau)\right)\partial_t(\widehat{Gu)(x},t_n)_l \\ &\quad -\frac{\varepsilon^2}{\alpha}\left(\int_0^\tau B_l(\tau-z)R_1\widehat{(x,t_n},z)_l\mathrm{d}z - P_l(\tau)R_2\widehat{(x,t_n})_l\right), \\ \widehat{\dot{\bar{\xi}}_l^{n+1}} &= -\frac{\varepsilon^2}{\alpha}\left(\int_0^1 D_l(\tau-z)\xi\mathrm{d}\xi - \frac{\tau}{2}Q_l(\tau)\right)\partial_t(\widehat{Gu)(x},t_n)_l \\ &\quad -\frac{\varepsilon^2}{\alpha}\left(\int_0^\tau D_l(\tau-z)R_1\widehat{(x,t_n},z)_l\mathrm{d}z - Q_l(\tau)R_2\widehat{(x,t_n})_l\right).\end{aligned} \tag{5.26}$$

Applying the boundedness of the function in Lemma 4.6 to the above formula gives

$$\begin{aligned}\big|\widehat{\bar{\xi}_l^{n+1}}\big| &\lesssim \varepsilon^2\tau^3\big|\partial_t(\widehat{Gu)(x},t_n)_l\big| + \varepsilon^2\left(\int_0^\tau \big|R_1\widehat{(x,t_n},z)_l\big|\mathrm{d}z + \tau\big|R_2\widehat{(x,t_n})_l\big|\right), \\ \big|\widehat{\dot{\bar{\xi}}_l^{n+1}}\big| &\lesssim \varepsilon^2\tau^3\big|\partial_t(\widehat{Gu)(x},t_n)_l\big| + \varepsilon^2\left(\int_0^\tau \big|R_1\widehat{(x,t_n},z)_l\big|\mathrm{d}z + \tau\big|R_2\widehat{(x,t_n})_l\big|\right).\end{aligned} \tag{5.27}$$

We define the local truncation error functions as

$$\bar{\xi}^{n+1}(x) = \sum_{l\in\Omega_M}\widehat{\bar{\xi}_l^{n+1}}\mathrm{e}^{i\mu_l(x-a)}, \quad \dot{\bar{\xi}}^{n+1}(x) = \sum_{l\in\Omega_M}\widehat{\dot{\bar{\xi}}_l^{n+1}}\mathrm{e}^{i\mu_l(x-a)}. \tag{5.28}$$

From the definition of the norm (2.3) and Cauchy inequality, we have the following H^m-estimates on $\bar{\xi}^{n+1}$ and H^{m-1}-estimates on $\dot{\bar{\xi}}^{n+1}$ as:

$$\begin{aligned}\|\bar{\xi}^{n+1}\|_m^2 &= \sum_{l\in\Omega_M}\big(1+|\mu_l|^2\big)^m\big|\widehat{\bar{\xi}_l^{n+1}}\big|^2 \\ &\lesssim \varepsilon^4\tau^6\sum_{l\in\Omega_M}\big(1+|\mu_l|^2\big)^m\big|\partial_t(\widehat{Gu)(x},t_n)_l\big| \\ &\quad + \varepsilon^4\sum_{l\in\Omega_M}\big(1+|\mu_l|^2\big)^m\left(\tau\int_0^\tau\big|R_1\widehat{(x,t_n},z)_l\big|^2\mathrm{d}z + \tau^2\big|R_2\widehat{(x,t_n})_l\big|^2\right) \\ &= \varepsilon^4\tau^6\|\partial_t(Gu)(x,t_n)\|_m^2 + \varepsilon^4\left(\tau\int_0^\tau\|R_1(x,t_n,z)\|_m^2\mathrm{d}z + \tau^2\|R_2(x,t_n)\|_m^2\right), \\ \|\dot{\bar{\xi}}^{n+1}\|_{m-1}^2 &= \sum_{l\in\Omega_M}\big(1+|\mu_l|^2\big)^{m-1}\big|\widehat{\dot{\bar{\xi}}_l^{n+1}}\big|^2 \\ &\lesssim \varepsilon^4\tau^6\sum_{l\in\Omega_M}\big(1+|\mu_l|^2\big)^{m-1}\big|\partial_t(\widehat{Gu)(x},t_n)_l\big| \\ &\quad + \varepsilon^4\sum_{l\in\Omega_M}\big(1+|\mu_l|^2\big)^{m-1}\left(\tau\int_0^\tau\big|R_1\widehat{(x,t_n},z)_l\big|^2\mathrm{d}z + \tau^2\big|R_2\widehat{(x,t_n})_l\big|^2\right) \\ &\lesssim \varepsilon^4\tau^6\big\|\partial_t(\widehat{Gu)(x},t_n)_l\big\|_{m-1}^2 \\ &\quad + \varepsilon^4\left(\tau\int_0^\tau\|R_1(x,t_n,z)\|_{m-1}^2\mathrm{d}z + \tau^2\|R_2(x,t_n)\|_{m-1}^2\right).\end{aligned} \tag{5.29}$$

From the assumption (A), Lemma 4.4 and (4.15), we get

$$\|\bar{\xi}^{n+1}\|_m^2 \lesssim \varepsilon^4\tau^6, \quad \|\dot{\bar{\xi}}^{n+1}\|_{m-1}^2 \lesssim \varepsilon^4\tau^6. \tag{5.30}$$

Step 2. Estimates on nonlinear errors. We subtract (5.7)-(5.8) from (5.16) and then get

$$\begin{aligned}\big(\widehat{\bar{e}_M^{n+1}}\big)_l &= A_l(\tau)\big(\widehat{\bar{e}_M^{n}}\big)_l + B_l(\tau)\big(\widehat{\dot{\bar{e}}_M^{n}}\big)_l + \widehat{\bar{\eta}_l^{n+1}} + \widehat{\bar{\xi}_l^{n+1}},\\ \big(\widehat{\dot{\bar{e}}_M^{n+1}}\big)_l &= C_l(\tau)\big(\widehat{\bar{e}_M^{n}}\big)_l + D_l(\tau)\big(\widehat{\dot{\bar{e}}_M^{n}}\big)_l + \widehat{\dot{\bar{\eta}}_l^{n+1}} + \widehat{\dot{\bar{\xi}}_l^{n+1}},\end{aligned} \tag{5.31}$$

where

$$\begin{aligned}\widehat{\bar{\eta}_l^{n+1}} &= -\frac{\varepsilon^2}{\alpha}P_l(\tau)\Big(G_B\big(u(x,\widehat{t_{n+1}), u}(x,t_n)\big)_l - G_B\big(I_M\widetilde{\bar{u}^{n+1}}, I_M\bar{u}^n\big)_l\Big),\\ \widehat{\dot{\bar{\eta}}_l^{n+1}} &= -\frac{\varepsilon^2}{\alpha}Q_l(\tau)\Big(G_B\big(u(x,\widehat{t_{n+1}), u}(x,t_n)\big)_l - G_B\big(I_M\widetilde{\bar{u}^{n+1}}, I_M\bar{u}^n\big)_l\Big).\end{aligned} \tag{5.32}$$

We introduce the nonlinear error for $n = 0, 1, \ldots, T_0\varepsilon^{-\beta}/\tau$

$$\bar{\eta}^{n+1}(x) = \sum_{l\in\Omega_M} \widehat{\bar{\eta}_l^{n+1}} \mathrm{e}^{i\mu_l(x-a)}, \quad \dot{\bar{\eta}}^{n+1}(x) = \sum_{l\in\Omega_M} \widehat{\dot{\bar{\eta}}_l^{n+1}} \mathrm{e}^{i\mu_l(x-a)}. \tag{5.33}$$

Using the bounds of $P_l(\tau)$ and $Q_l(\tau)$ in Lemma 4.6 and the definition of (2.3), we obtain

$$\|\bar{\eta}^{n+1}\|_m \lesssim \varepsilon^2\tau\|R\|_m, \quad \|\dot{\bar{\eta}}^{n+1}\|_{m-1} \lesssim \varepsilon^2\tau\|R\|_{m-1}, \tag{5.34}$$

where

$$R = P_M G_B\big(u(x,t_{n+1}), u(x,t_n)\big) - I_M G_B\big(I_M\bar{u}^{n+1}, I_M\bar{u}^n\big).$$

From (4.12), (4.13) and (5.11), we get

$$\begin{aligned}\|R\|_{m-1} \le \|R\|_m &\le \big\|I_M G_B\big(u(x,t_{n+1}), u(x,t_n)\big) - I_M G_B\big(I_M\bar{u}^{n+1}, I_M\bar{u}^n\big)\big\|_m\\ &\quad + Ch^{m_0}\big\|G_B\big(u(x,t_{n+1}), u(x,t_n)\big)\big\|_{m+m_0}\\ &\lesssim \big\|G_B\big(u(x,t_{n+1}), u(x,t_n)\big) - G_B\big(I_M\bar{u}^{n+1}, I_M\bar{u}^n\big)\big\|_m + h^{m_0}\\ &\lesssim \|\bar{e}^{n+1}\|_m + \|\bar{e}^n\|_m + h^{m_0}\\ &\lesssim \big\|\bar{e}_M^{n+1}\big\|_m + \big\|\bar{e}_M^n\big\|_m + h^{m_0}.\end{aligned} \tag{5.35}$$

Plugging (5.35) into (5.34) immediately leads to

$$\begin{aligned}\|\bar{\eta}^{n+1}\|_m^2 &\lesssim \varepsilon^4\tau^2\left(\big\|\bar{e}_M^n\big\|_m^2 + \big\|\bar{e}_M^{n+1}\big\|_m^2 + h^{2m_0}\right),\\ \|\dot{\bar{\eta}}^{n+1}\|_{m-1}^2 &\lesssim \varepsilon^4\tau^2\left(\big\|\bar{e}_M^n\big\|_m^2 + \big\|\bar{e}_M^{n+1}\big\|_m^2 + h^{2m_0}\right).\end{aligned} \tag{5.36}$$

Step 3. Error equations on $\bar{e}_M^n$ and $\dot{\bar{e}}_M^n$. Firstly we consider the case $\alpha > 0$. It follows from (5.31) that

$$\begin{aligned}\big|\big(\widehat{\bar{e}_M^{n+1}}\big)_l\big|^2 &\lesssim (1+\varepsilon^\beta\tau)\Big|A_l(\tau)\big(\widehat{\bar{e}_M^{n}}\big)_l + B_l(\tau)\big(\widehat{\dot{\bar{e}}_M^{n}}\big)_l\Big|^2 + \left(1+\frac{1}{\varepsilon^\beta\tau}\right)\left(\big|\widehat{\bar{\eta}_l^{n+1}}\big|^2 + b\widehat{\bar{\xi}_l^{n+1}}^2\right),\\ \big|\big(\widehat{\dot{\bar{e}}_M^{n+1}}\big)_l\big| &\lesssim (1+\varepsilon^\beta\tau)\Big|C_l(\tau)\big(\widehat{\bar{e}_M^{n}}\big)_l + D_l(\tau)\big(\widehat{\dot{\bar{e}}_M^{n}}\big)_l\Big|^2 + \left(1+\frac{1}{\varepsilon^\beta\tau}\right)\left(\big|\widehat{\dot{\bar{\eta}}_l^{n+1}}\big|^2 + \big|\widehat{\dot{\bar{\xi}}_l^{n+1}}\big|^2\right).\end{aligned}$$

Adding the first formula to the second one multiplied by α/μ_l^2, we obtain

$$\begin{aligned}&\big|\big(\widehat{\bar{e}_M^{n+1}}\big)_l\big|^2 + \frac{\alpha}{\mu_l^2}\big|\big(\widehat{\dot{\bar{e}}_M^{n+1}}\big)_l\big|^2\\ &\lesssim (1+\varepsilon^\beta\tau)\left(\big|\big(\widehat{\bar{e}_M^{n}}\big)_l\big|^2 + \frac{\alpha}{\mu_l^2}\big|\big(\widehat{\dot{\bar{e}}_M^{n}}\big)_l\big|^2\right)\\ &\qquad + \left(1+\frac{1}{\varepsilon^\beta\tau}\right)\left(\big|\widehat{\bar{\eta}_l^{n+1}}\big|^2 + \big|\widehat{\bar{\xi}_l^{n+1}}\big|^2 + \frac{\alpha}{\mu_l^2}\big|\widehat{\dot{\bar{\eta}}_l^{n+1}}\big|^2 + \frac{\alpha}{\mu_l^2}\big|\widehat{\dot{\bar{\xi}}_l^{n+1}}\big|^2\right).\end{aligned} \tag{5.37}$$

From the definition (2.3), it is easy to get

$$\begin{aligned}&\left\|\bar{e}_M^{n+1}\right\|_m^2+\alpha\left\|\dot{\bar{e}}_M^{n+1}\right\|_{m-1}^2\\ &\le(1+\varepsilon^\beta\tau)\Big(\left\|\bar{e}_M^n\right\|_{m^*}^2+\alpha\left\|\dot{\bar{e}}_M^n\right\|_{m-1}^2\Big)\\ &\quad+\left(1+\frac{1}{\varepsilon^\beta\tau}\right)\Big(\left\|\bar{\eta}_l^{n+1}\right\|_m^2+\left\|\bar{\xi}_l^{n+1}\right\|_m^2+\alpha\left\|\dot{\bar{\eta}}^{n+1}\right\|_{m-1}^2+\alpha\left\|\dot{\bar{\xi}}_l^{n+1}\right\|_{m-1}^2\Big).\end{aligned} \tag{5.38}$$

Plugging (5.30) and (5.36) into (5.38), it is easy to get

$$\begin{aligned}\left\|\bar{e}_M^{n+1}\right\|_{m^*}^2+\alpha\left\|\dot{\bar{e}}_M^{n+1}\right\|_{m-1}^2\lesssim&\Big(\left\|\bar{e}_M^n\right\|_{m^*}^2+\alpha\left\|\dot{\bar{e}}_M^n\right\|_{m-1}^2\Big)\\ &+\varepsilon^\beta\tau\Big(\left\|\bar{e}_M^{n+1}\right\|_m^2+\left\|\bar{e}_M^n\right\|_m^2+\alpha\left\|\dot{\bar{e}}_M^n\right\|_{m-1}^2\Big)\\ &+\varepsilon^{4-\beta}\tau h^{2m_0}+\varepsilon^{4-\beta}\tau^5,\end{aligned} \tag{5.39}$$

where $\varepsilon^{4-\beta}\le\varepsilon^\beta$ has been used. Define the energy

$$\mathcal{E}^n=\left\|\bar{e}_M^n\right\|_{m^*}^2+\alpha\left\|\dot{\bar{e}}_M^n\right\|_m^2. \tag{5.40}$$

From (5.39) and the definition of the energy (5.40), we obtain

$$\mathcal{E}^{n+1}-\mathcal{E}^n\lesssim\tau(\mathcal{E}^{n+1}+\mathcal{E}^n)+\varepsilon^{4-\beta}\tau h^{2m_0}+\varepsilon^{4-\beta}\tau^5,\quad n=0,\dots,T_0\varepsilon^{-\beta}/\tau-1. \tag{5.41}$$

Summing up (5.41) for $n=1,\dots,k$, using (5.34), we derive

$$\mathcal{E}^{k+1}-\mathcal{E}^0\lesssim\tau\sum_{j=1}^{k+1}\mathcal{E}^j+\varepsilon^{4-2\beta}h^{2m_0}+\varepsilon^{4-2\beta}\tau^4,\quad k=0,\dots,T_0\varepsilon^{-\beta}/\tau-1. \tag{5.42}$$

Obviously, we have

$$\left\|\bar{e}_M^0\right\|_m\lesssim h^{m_0},\quad\left\|\dot{\bar{e}}_M^0\right\|_{m-1}\lesssim h^{m_0}. \tag{5.43}$$

Using the discrete Gronwall's lemma to the above inequality, we can conclude that there exist sufficiently small values $h_1>0$ and $\tau_1>0$, when $0<h\le h_1$ and $0<\tau\le\varepsilon^{1-\beta/2}\tau_1$, it is hold that

$$\mathcal{E}^{k+1}\lesssim h^{2m_0}+\varepsilon^{4-2\beta}\tau^4,\quad k=0,\dots,T_0\varepsilon^{-\beta}/\tau-1. \tag{5.44}$$

From the inequality $\sqrt{a+b}\le\sqrt{a}+\sqrt{b}$ and the definition of energy in (5.40), we have

$$\left\|e_M^n\right\|_m\lesssim h^{m_0}+\varepsilon^{2-\beta}\tau^2,\quad\left\|\dot{\bar{e}}_M^n\right\|_m\lesssim h^{m_0}+\varepsilon^{2-\beta}\tau^2. \tag{5.45}$$

From (5.45), we have

$$\begin{aligned}\|\bar{e}^n\|_m&\lesssim\left\|e_M^n\right\|_m+h^{m_0}\lesssim h^{m_0}+\varepsilon^{2-\beta}\tau^2,\\ \|\dot{\bar{e}}^n\|_m&\lesssim\left\|\dot{\bar{e}}_M^n\right\|_m+h^{m_0}\lesssim h^{m_0}+\varepsilon^{2-\beta}\tau^2.\end{aligned} \tag{5.46}$$

It follows from (5.46) that for sufficiently small constants $h_2>0$ and $\tau_2>0$, when $0<h\le h_2$ and $0<\tau\le\varepsilon^{1-\beta/2}\tau_2$, the following result holds:

$$\begin{aligned}\left\|I_M\bar{u}^n\right\|_m&\le\|\bar{e}^n\|_m+\|u(x,t_n)\|_m\le 1+M_u,\\ \left\|I_M\dot{\bar{u}}^n\right\|_{m-1}&\le\|\dot{\bar{e}}^n\|_{m-1}+\|\partial_t u(x,t_n)\|_{m-1}\le 1+M_u'.\end{aligned} \tag{5.47}$$

Thus, if we take $h_0=\min\{h_1,h_2\}$ and $\tau_0=\min\{\tau_1,\tau_2\}$, the theorem holds. □

From the definition (5.4), we know that for such τ_0 and h_0, the modified EWIFP method (5.6) with (5.7)-(5.8) collapses exactly to the SEPEWIFP method. Thus, the proof of Theorem 5.1 is complete.

Remark 5.2. We can extend the SEPEWIFP method and corresponding error estimates to the NLSW with a general power nonlinearity $\varepsilon^{2p}|u(\mathbf{x},t)|^{2p}u(\mathbf{x},t)$. For one-dimensional problems, we only need replace (2.21) with the following formula:

$$G(u^{n+1},u^n)_j = \frac{\left|u_j^{n+1}\right|^{2(p+1)} - \left|u_j^n\right|^{2(p+1)}}{\left|u_j^{n+1}\right|^2 - \left|u_j^n\right|^2} \frac{\left(u_j^{n+1}+u_j^n\right)}{2(p+1)}. \tag{5.48}$$

Furthermore, for the more general nonlinearity $\varepsilon f(|u(\mathbf{x},t)|^2)u(\mathbf{x},t)$, we can also construct our method. In one-dimensionalcase, we only need replace (2.21) with the following formula:

$$G(u^{n+1},u^n)_j = \int_0^1 f\left(\theta\left|u_j^{n+1}\right|^2 + (1-\theta)\left|u_j^n\right|^2\right) \mathrm{d}\theta \frac{\left(u_j^{n+1}+u_j^n\right)}{2}. \tag{5.49}$$

The relevant analysis is completely similar to the analysis in this paper and will not be made in detail here due to space limitations. In particular, when $f(v) = -v$, we obtain the nonlinearity in the defocusing case and express (2.2) as $G(u) = -|u|^2u$.

6. Numerical Results

In this section we present numerical results for the SEPEWIFP method for the NLSW with weak nonlinearity.

6.1. The one-dimensional problem

Since the method is implicit, here we specify how to solve the nonlinear equation in practical computation. Since (2.19) is implicit, we evaluate u^{n+1} through fixed point iteration. Firstly, for a given u^n, we provide an explicit approximation $u^{n+1,0}$ of $u(x,t_{n+1})$ by an explicit method and then we use the iteration

$$\begin{aligned}
(\widetilde{u^{n+1,k+1}})_l &= A_l(\tau)(\widetilde{u^n})_l + B_l(\tau)(\widetilde{\dot{u}^n})_l - \frac{\varepsilon^2}{\alpha}P_l(\tau)G(\widetilde{u^{n+1,k}},u^n)_l,\\
u_j^{n+1,k+1} &= \sum_{l\in\Omega_M} (\widetilde{u^{n+1,k+1}})_l e^{\frac{2ijl\pi}{M}}, \quad k = 0,1,\ldots.
\end{aligned}$$

Giving a tolerance Tol, when $\|u^{n+1,k+1} - u^{n+1,k}\|_{l^2} \le Tol$, the program stops and we take $u^{n+1} = u^{n+1,k+1}$. Then $\dot{u}^{n+1}$ can be calculated directly because that (2.20) is explicit.

In our numerical tests, we choose $\alpha = 1$, computational domain $\Omega = [-\pi,\pi]$, and initial data in the NLSW (2.1) as

$$u_0(x) = \frac{1}{2+\cos^2(x)+\sin(x)}, \quad u_1(x) = \frac{1}{2+\sin^2(x)+\cos(x)}, \quad x\in[-\pi,\pi]. \tag{6.1}$$

In order to describe the error, we take

$$\|e(\cdot,t_n)\|_m = \left\|u(\cdot,t_n) - u^n\right\|_m + \left\|u(\cdot,t_n) - u^n\right\|_{m-1},$$

where $u(x,t)$ and $\partial_t u(x,t)$ are the exact solution and its derivative, respectively. Here we only take $m = 1$ as examples and do not consider $m \geq 2$ in that case the results are similar. The time intervals are $[0, 1/\varepsilon^\beta]$ with $\beta = 0, 1, 2$, respectively.

Tables 6.1-6.3 shows the temporal errors of the SEPEWIFP method under different ε and τ with $h = \pi/2^5$. We describe the numerical results by $\|e(\cdot, 1/\varepsilon^\beta)\|_1/\varepsilon^{2-\beta}$ for reflecting that the temporal errors are $O(\varepsilon^{2-\beta}\tau^2)$, Table 6.4 shows the spatial errors of the SEPEWIFP method under different ε and h with $\tau = 10^{-4}$.

Numerically describing energy-preservation of the method is necessary and interesting. In order to describe the long-term behavior of energy errors for the SEPEWIFP method, we take the long enough computational interval $[0, 1000]$, lager mesh size $h = \pi/4$ and time step $\tau = 0.2$. In this case the error of the numerical solution tends to be large due to the long-term accumulation. The discrete energy are shown in Fig. 6.1. It should be noted that some minor errors appear in Fig. 6.1. This is mainly because of the iterative process included and discrete Fourier transform (FFT).

Table 6.1: Temporal error of the SEPEWIFP method for different ε and τ with $\beta = 0$.

$\|e(\cdot,1/\varepsilon^\beta)\|_1/\varepsilon^{2-\beta}$	$\tau_0 = 0.2$	$\tau_0/2$	$\tau_0/2^2$	$\tau_0/2^3$	$\tau_0/2^4$	$\tau_0/2^5$
$\varepsilon_0 = 1$	1.27E-2	3.28E-3	8.28E-4	2.07E-4	5.19E-5	1.29E-5
order	–	1.95	1.99	2.00	2.00	2.00
$\varepsilon_0/2$	6.75E-3	1.71E-3	4.28E-4	1.07E-4	2.68E-5	6.70E-6
order	–	1.98	2.00	2.00	2.00	2.00
$\varepsilon_0/2^2$	5.36E-3	1.35E-3	3.37E-4	8.43E-5	2.11E-5	5.27E-6
order	–	1.99	2.00	2.00	2.00	2.00
$\varepsilon_0/2^3$	4.98E-3	1.25E-4	3.12E-4	7.81E-5	1.95E-5	4.88E-6
order	–	2.00	2.00	2.00	2.00	2.00
$\varepsilon_0/2^4$	4.83E-3	1.21E-3	3.03E-4	7.57E-5	1.89E-5	4.73E-6
order	–	2.00	2.00	2.00	2.00	2.00
$\varepsilon_0/2^5$	4.76E-3	1.19E-3	2.98E-4	7.46E-5	1.87E-5	4.66E-6
order	–	2.00	2.00	2.00	2.00	2.00

Table 6.2: Temporal error of the SEPEWIFP method for different ε and τ with $\beta = 1$.

$\|e(\cdot,1/\varepsilon^\beta)\|_1/\varepsilon^{2-\beta}$	$\tau_0 = 0.2$	$\tau_0/2$	$\tau_0/2^2$	$\tau_0/2^3$	$\tau_0/2^4$	$\tau_0/2^5$
$\varepsilon_0 = 1$	1.27E-2	3.28E-3	8.28E-4	2.07E-4	5.19E-5	1.30E-5
order	–	1.95	1.99	2.00	2.00	2.00
$\varepsilon_0/2$	9.51E-3	2.40E-3	6.03E-4	1.51E-4	3.77E-5	9.42E-6
order	–	1.98	2.00	2.00	2.00	2.00
$\varepsilon_0/2^2$	1.17E-2	2.94E-3	7.36E-4	1.84E-4	4.60E-5	1.15E-5
order	–	1.99	2.00	2.00	2.00	2.00
$\varepsilon_0/2^3$	6.97E-3	1.75E-3	4.37E-4	1.09E-4	2.73E-5	6.83E-6
order	–	2.00	2.00	2.00	2.00	2.00
$\varepsilon_0/2^4$	9.33E-3	2.34E-3	5.86E-4	1.47E-4	3.67E-5	9.16E-6
order	–	1.99	2.00	2.00	2.009	2.00
$\varepsilon_0/2^5$	9.59E-3	2.41E-3	6.02E-4	1.51E-4	3.77E-5	9.41E-6
order	–	1.99	2.00	2.00	2.00	2.00

Table 6.3: Temporal error of the SEPEWIFP method for different ε and τ with $\beta = 2$.

$\|e(\cdot, 1/\varepsilon^\beta)\|_1/\varepsilon^{2-\beta}$	$\tau_0 = 0.2$	$\tau_0/2$	$\tau_0/2^2$	$\tau_0/2^3$	$\tau_0/2^4$	$\tau_0/2^5$
$\varepsilon_0 = 1$	1.27E-2	3.28E-3	8.27E-4	2.07E-4	5.19E-5	1.30E-5
order	–	1.95	1.99	2.00	2.00	2.00
$\varepsilon_0/2$	8.69E-3	2.19E-3	5.49E-4	1.37E-4	3.43E-5	8.58E-6
order	–	1.99	2.00	2.00	2.00	2.00
$\varepsilon_0/2^2$	9.51E-3	2.39E-3	5.98E-4	1.50E-4	3.74E-5	9.35E-6
order	–	1.99	2.00	2.00	2.00	2.00
$\varepsilon_0/2^3$	7.93E-3	1.99E-3	4.99E-4	1.25E-4	3.12E-5	7.79E-6
order	–	1.99	2.00	2.00	2.00	2.00
$\varepsilon_0/2^4$	9.85E-3	2.47E-3	6.18E-4	1.55E-4	3.86E-5	9.66E-6
order	–	1.99	2.00	2.00	2.00	2.00
$\varepsilon_0/2^5$	7.13E-3	1.79E-3	4.47E-4	1.12E-4	2.79E-5	6.98E-6
order	–	2.00	2.00	2.00	2.00	2.00

Table 6.4: Spatial error of the SEPEWIFP method for different ε and h with $\beta = 0, 1, 2$, respectively.

	$\|e(\cdot, 1/\varepsilon^\beta)\|_1$	$h_0 = \pi/2$	$h_0/2$	$h_0/2^2$	$h_0/2^3$
$\beta = 0$	$\varepsilon_0 = 1$	1.05E-1	9.40E-3	4.69E-5	4.98E-10
	$\varepsilon_0/2$	1.07E-1	8.60E-3	4.49E-5	5.09E-10
	$\varepsilon_0/2^2$	1.08E-1	8.38E-3	4.40E-5	5.07E-10
	$\varepsilon_0/2^3$	1.08E-1	8.32E-3	4.38E-5	5.06E-10
	$\varepsilon_0/2^4$	1.08E-1	8.31E-3	4.37E-5	5.06E-10
$\beta = 1$	$\varepsilon_0 = 1$	1.05E-1	9.40E-3	4.69E-5	4.98E-10
	$\varepsilon_0/2$	1.01E-1	9.92E-3	4.75E-5	4.33E-10
	$\varepsilon_0/2^2$	9.98E-2	9.86E-3	4.05E-5	4.86E-10
	$\varepsilon_0/2^3$	1.12E-1	9.33E-3	5.17E-5	3.98E-10
	$\varepsilon_0/2^4$	3.82E-2	3.29E-3	1.53E-5	1.76E-10
$\beta = 2$	$\varepsilon_0 = 1$	1.05E-1	9.40E-3	4.69E-5	4.98E-10
	$\varepsilon_0/2^1$	1.02E-1	9.85E-3	3.80E-5	4.84E-10
	$\varepsilon_0/2^2$	3.59E-2	3.04E-3	1.56E-5	2.27E-10
	$\varepsilon_0/2^3$	7.94E-2	9.99E-3	4.69E-5	3.87E-10
	$\varepsilon_0/2^4$	8.60E-2	1.04E-2	4.11E-5	4.94E-10

In addition, with the same data, we also show long-term stability of the discrete mass of the SEPEWIFP method in Fig. 6.2. Here we take the discrete mass as

$$M^n := \|u^n\|_{l^2}^2 - 2h \sum_{j=0}^{M-1} \mathrm{Im}\big[\,\overline{u_j^n}\dot{u}_j^n\big], \quad n = 0, 1, \ldots, \tag{6.2}$$

where

$$\|u\|_{l^2}^2 = h \sum_{j=0}^{M-1} |u_j|^2.$$

From Tables 6.1-6.4 and Figs. 6.1-6.2, the following observations on the SEPEWIFP method for the NLSW (2.1) can be drawn:

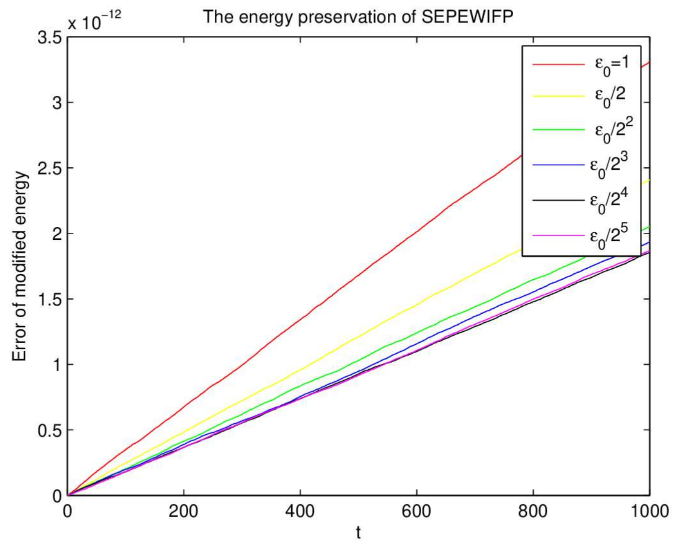

Fig. 6.1. Energy preservation of SEPEWIFP.

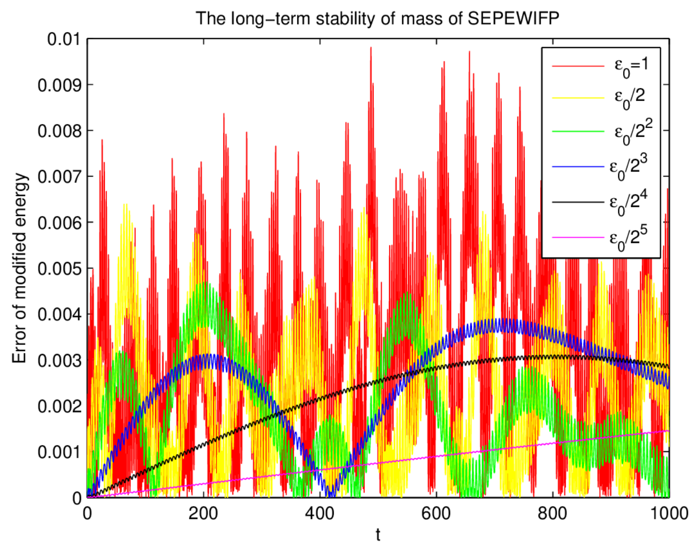

Fig. 6.2. Long-term stability of mass of SEPEWIFP.

(i) The temporal errors of the SEPEWIFP method behave like $\mathcal{O}(\varepsilon^{2-\beta}\tau^2)$ up to the time at $\mathcal{O}(\varepsilon^{-\beta})$ (see Tables 6.1-6.3).

(ii) The spatial errors of the SEPEWIFP method are $\mathcal{O}(h^{m_0})$ which imply that the method is uniformly spectrally accurate for any $\varepsilon \in (0, 1]$ and $\beta \in [0, 2]$ (see each row in Table 6.4).

(iii) The discrete energy is preserved along the numerical solution of the SEPEWIFP method for the NLSW (2.1) (see Fig. 6.1). This verifies that the conclusion of Theorem 4.1 is correct.

(iv) The numerical solution still exhibits good convergence without a CFL-type stability condition.

(v) Although this method does not preserve the mass, it exhibits good long-term stability of the discrete mass (see Fig. 6.2).

In summary, numerous numerical results strongly confirm the correctness of our theoretical analysis in this paper.

6.2. A higher-dimensional problem

Due to space limitations, we only consider a 2D NLSW (1.1). Here we take $\Omega = [0, 2\pi] \times [0, 2\pi], T_0 = 1$ and the initial condition

$$u^0(x, y) = \frac{1}{4 + \cos^2(x) + \cos^2(y)}, \quad \dot{u}^0(x, y) = \sin(x) + \sin(y).$$

We only take $\beta = 2$ which can better reflect the long time error of the numerical solution. Table 6.5 shows the temporal errors of the method at $t = T_0/\varepsilon^\beta$ under different τ with a small mesh size $h = \pi/2^6$. Table 6.6 shows the spatial errors of the method at $t = T_0/\varepsilon^\beta$ under different h with a very small time step $\tau = 10^{-4}$.

In order to describe the long-term behavior of energy errors and mass errors for the method, we take the long enough time interval $[0, 1000]$, lager mesh size $h = \pi/2$ and time step $\tau = 0.1$. The discrete energy-preservation and long-term stability of mass for SEPEWIFP are shown in Figs. 6.3 and 6.4, respectively.

Table 6.5: Temporal errors of SEPEWIFP for the 2D NLSW (1.1) with different ε and τ for $\beta = 2$.

$\Vert e(\cdot, 1/\varepsilon^\beta)\Vert_2$	$\tau_0 = 0.1$	$\tau_0/2$	$\tau_0/2^2$	$\tau_0/2^3$	$\tau_0/2^4$	$\tau_0/2^5$
$\varepsilon_0 = 1$	4.11E-3	1.04E-3	2.59E-4	6.48E-5	1.62E-5	4.05E-6
order	–	1.99	2.00	2.00	2.00	2.00
$\varepsilon_0/2$	4.03E-3	1.01E-3	2.53E-4	6.32E-5	1.58E-5	3.95E-6
order	–	2.00	2.00	2.00	2.00	2.00
$\varepsilon_0/2^2$	5.27E-3	1.32E-3	3.30E-4	8.25E-5	2.06E-5	5.15E-6
order	–	2.00	2.00	2.00	2.00	2.00
$\varepsilon_0/2^3$	5.49E-3	1.37E-3	3.44E-4	8.59E-5	2.15E-5	5.37E-6
order	–	2.00	2.00	2.00	2.00	2.00
$\varepsilon_0/2^4$	4.98E-3	1.25E-3	3.11E-4	7.79E-5	1.95E-5	4.86E-6
order	–	2.00	2.00	2.00	2.00	2.00
$\varepsilon_0/2^5$	3.24E-3	1.63E-3	3.41E-4	7.53E-5	1.82E-5	4.20E-6
order	–	1.99	2.00	2.00	2.00	2.00

Table 6.6: Spatial errors of SEPEWIFP for the 2D NLSW (1.1) with different ε and h for $\beta = 2$.

$\Vert e(\cdot, 1/\varepsilon^\beta)\Vert_2$	$h_0 = \pi/2$	$h_0/2$	$h_0/2^2$	$h_0/2^3$
$\varepsilon_0 = 1$	1.79E-2	4.55E-4	2.82E-6	4.73E-11
$\varepsilon_0/2$	4.86E-2	1.05E-3	3.44E-6	4.82E-11
$\varepsilon_0/2^2$	9.39E-2	4.19E-4	1.37E-6	2.70E-11
$\varepsilon_0/2^3$	1.09E-1	4.97E-4	2.27E-6	5.83E-11
$\varepsilon_0/2^4$	1.05E-1	4.63E-4	2.58E-6	1.87E-10

Numerical results from Tables 6.5-6.6 and Figs. 6.3-6.4 strongly confirm the correctness of our theoretical results for higher-dimensional KGD equation. This means that the conclusions drawn from one-dimensional KGD equation also apply to higher-dimensional KGD equations.

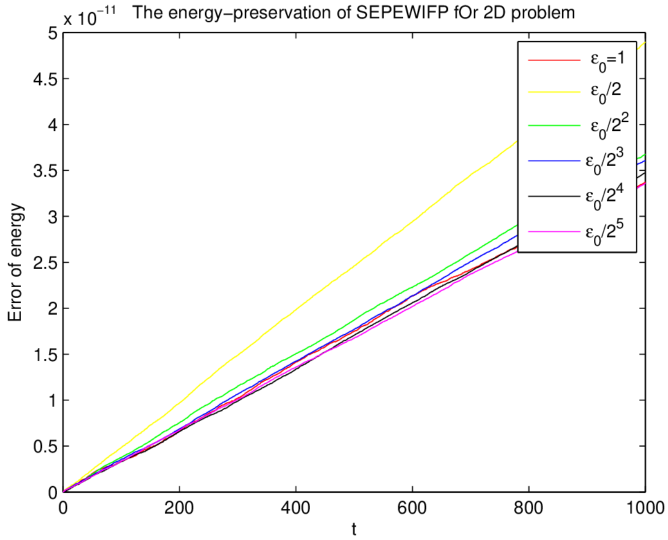

Fig. 6.3. Energy preservation of SEPEWIFP for 2D problem.

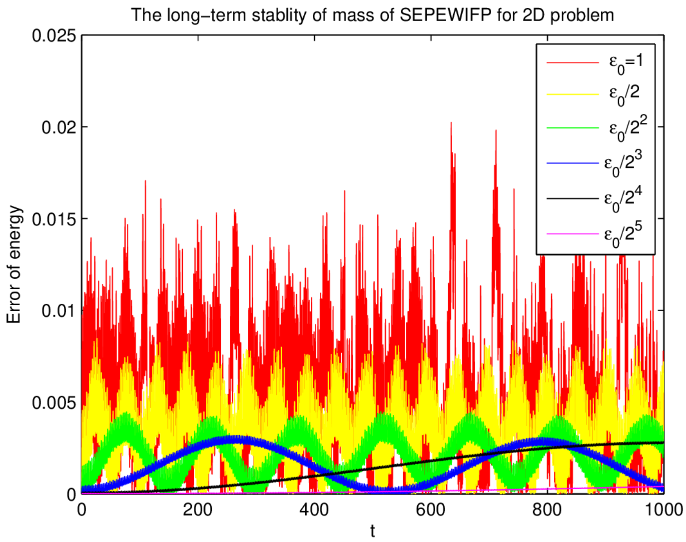

Fig. 6.4. Long-term stability of mass of SEPEWIFP for 2D problem.

7. Extension to an Oscillatory NLSW

In the NLSW (1.1), taking $s = \varepsilon^{\beta} t$ with $0 \leq \beta \leq 2$ and $v(\mathbf{x}, s) = u(\mathbf{x}, s/\varepsilon^{\beta})$, we obtain the equivalent problem

$$\begin{cases} i\varepsilon^{\beta}\partial_s v(\mathbf{x},s) - \alpha\varepsilon^{2\beta}\partial_{ss}v(\mathbf{x},s) + \Delta v(\mathbf{x},s) - \varepsilon^2|v(\mathbf{x},s)|^2 v(\mathbf{x},s) = 0, & x \in \mathbb{T}^d, \quad s > 0, \\ v(\mathbf{x},0) = u_0(\mathbf{x}), \quad \partial_s v(\mathbf{x},0) = \varepsilon^{-\beta}u_1(\mathbf{x}), & x \in \mathbb{T}^d, \end{cases} \tag{7.1}$$

which has the time symmetry and preserves the mass and energy as

$$\begin{aligned} \bar{M}(s) &:= \varepsilon^{\beta}\int_{\mathbb{T}^d}|v(\mathbf{x},s)|^2 \mathrm{d}\mathbf{x} - 2\varepsilon^{2\beta}\alpha\int_{\mathbb{T}^d}\mathrm{Im}\left[\overline{v(\mathbf{x},s)}\partial_t v(\mathbf{x},s)\right]\mathrm{d}\mathbf{x} = \bar{M}(0), \quad s \geq 0 \\ \bar{E}(s) &:= \int_{T^d}\left[\alpha\varepsilon^{2\beta}|\partial_s v(\mathbf{x},s)|^2 + |\nabla v(\mathbf{x},s)|^2 + \frac{\varepsilon^2}{2}|v(\mathbf{x},s)|^4\right]\mathrm{d}\mathbf{x} =: \bar{E}(0), \quad s \geq 0. \end{aligned} \tag{7.2}$$

Plugging the plane wave solution $v(\mathbf{x},s) = Ae^{i(\mathbf{k}\cdot\mathbf{x}-\omega s)}$ (with ω the time frequency, A the amplitude and $\mathbf{k} = (k_1,\cdots,k_d)^T \in \mathbb{R}^d$ the spatial wave number) into (7.1), we obtain the following dispersion relation:

$$\alpha\varepsilon^{2\beta}\omega^2 + \varepsilon^{\beta}\omega - |\mathbf{k}|^2 - \varepsilon^2 A^2 = 0, \tag{7.3}$$

which immediately implies the time frequency

$$\omega := \omega(\mathbf{k}) = \frac{1}{2\alpha\varepsilon^{\beta}}\left(-1 + \sqrt{1 + 4\alpha(|\mathbf{k}|^2 + \varepsilon^2 A^2)}\right) = \mathcal{O}\left(\varepsilon^{-\beta}\right), \tag{7.4}$$

and further implies the group velocity

$$v := v(\mathbf{k}) = \nabla\omega(\mathbf{k}) = \frac{2|\mathbf{k}|}{\varepsilon^{\beta}\sqrt{1 + 4\alpha(|\mathbf{k}|^2 + \varepsilon^2 A^2)}} = \mathcal{O}\left(\varepsilon^{-\beta}\right). \tag{7.5}$$

Thus, the solution of the NLSW (7.1) propagates waves with amplitude at $\mathcal{O}(1)$, wavelength at $\mathcal{O}(1)$ in space and $\mathcal{O}(\varepsilon^{\beta})$ in time, respectively, and wave velocity at $\mathcal{O}(\varepsilon^{-\beta})$.

Again, we only consider the 1D problem. For high-dimensional problems, the proposal of the method, the proof of the structure preservation and the error analysis are all similar to the 1D problem. In 1D, the NLSW (7.1) with periodic boundary conditions collapses to

$$\begin{aligned} & i\varepsilon^{\beta}\partial_s v(x,s) - \alpha\varepsilon^{2\beta}\partial_{ss}v(x,s) + \partial_{xx}v(x,s) - \varepsilon^2|v(x,s)|^2 v(x,s) = 0, && x \in \Omega, \quad s > 0, \\ & v(a,s) = v(b,s), \quad \partial_x v(a,s) = \partial_x v(b,s), && s \geq 0, \\ & v(x,0) = u_0(x), \quad \partial_s v(x,0) = \varepsilon^{-\beta}u_1(x), && x \in \bar{\Omega}, \end{aligned} \tag{7.6}$$

where $\Omega = (a,b)$.

7.1. SEPEWIFP method

Choose the time step $k := \Delta s > 0$ and denote grid points as $s_n := nk$ for $n = 0,1,\ldots$. For $l \in \Omega_M$, we take a_l as in (2.11) and denote

$$\gamma = \varepsilon^{\beta}\alpha. \tag{7.7}$$

Introduce

$$\begin{aligned} \mathcal{A}_l(s) &= \mathrm{e}^{is/(2\gamma)}\left(\cos\left(\frac{sa_l}{2\gamma}\right) - \frac{i}{a_l}\sin\left(\frac{sa_l}{2\gamma}\right)\right), \\ \mathcal{B}_l(s) &= \mathrm{e}^{is/(2\gamma)}\frac{2\gamma}{a_l}\sin\left(\frac{sa_l}{2\gamma}\right), \\ \mathcal{C}_l(s) &= -\mathrm{e}^{is/(2\gamma)}\frac{2\mu^2}{\varepsilon^{\beta}a_l}\sin\left(\frac{sa_l}{2\gamma}\right), \\ \mathcal{D}_l(s) &= \mathrm{e}^{is/(2\gamma)}\left(\cos\left(\frac{sa_l}{2\gamma}\right) + \frac{i}{a_l}\sin\left(\frac{sa_l}{2\gamma}\right)\right). \end{aligned} \tag{7.8}$$

In order to construct the energy-preseving method, we define the functions $\mathcal{P}_l(s)$ and $\mathcal{Q}_l(s)$ as

$$\mathcal{P}_l(s) = \int_0^s \mathcal{B}_l(s-z)\mathrm{d}z, \quad \mathcal{Q}_l(s) = \int_0^s \mathcal{D}_l(s-z)\mathrm{d}z. \tag{7.9}$$

The functions $\mathcal{P}_l(s)$ and $\mathcal{Q}_l(s)$ are continuous with respect to s. Direct calculation gives

$$\begin{aligned} &\mathcal{P}_l(s) = \begin{cases} \dfrac{\alpha\varepsilon^{2\beta}}{\mu_l^2}\left(1 - \mathrm{e}^{\frac{is}{2\gamma}}\left(\cos\left(\dfrac{sa_l}{2\gamma}\right) - \dfrac{i}{a_l}\sin\left(\dfrac{sa_l}{2\gamma}\right)\right)\right), & \mu_l \neq 0, \\ \gamma\big(\gamma - \gamma\mathrm{e}^{\frac{is}{\gamma}} + is\big), & \mu_l = 0, \end{cases} \\ &Q_l(s) = \mathrm{e}^{\frac{is}{2\gamma}}\frac{2\gamma}{a_l}\sin\left(\frac{sa_l}{2\gamma}\right). \end{aligned} \tag{7.10}$$

The derivation process of the SEPEWIFP method for the NLSW (7.6) is similar to the one in Section 2. Let v_j^n and $\dot{v}_j^n$ $(j = 0, \ldots, M)$ be the approximations of $v(x_j, s_n)$ and $\partial_s v(x_j, s_n)$, respectively. Choose $v_j^0 = u_0(x_j)$ and $\dot{v}_j^0 = \varepsilon^{-\beta}u_1(x_j)$, then for $n = 0, 1, \ldots,$ a SEPEWIFP discretization for the NLSW (7.6) is

$$v_j^{n+1} = \sum_{l\in\Omega_M} \widetilde{(v^{n+1})}_l \mathrm{e}^{\frac{2ijl\pi}{M}}, \quad \dot{v}_j^{n+1} = \sum_{l\in\Omega_M} \widetilde{(\dot{v}^{n+1})}_l \mathrm{e}^{\frac{2ijl\pi}{M}}, \tag{7.11}$$

where

$$\begin{aligned} \widetilde{(v^{n+1})}_l &= \mathcal{A}_l(k)\widetilde{(v^n)}_l + \mathcal{B}_l(k)\widetilde{(\dot{v}^n)}_l - \frac{\varepsilon^{2-2\beta}}{\alpha}\mathcal{P}_l(k)\widetilde{G(v^{n+1}, v^n)}_l, \\ \widetilde{(\dot{v}^{n+1})}_l &= \mathcal{C}_l(k)\widetilde{(v^n)}_l + \mathcal{D}_l(k)\widetilde{(\dot{v}^n)}_l - \frac{\varepsilon^{2-2\beta}}{\alpha}\mathcal{Q}_l(k)\widetilde{G(v^{n+1}, v^n)}_l, \end{aligned} \tag{7.12}$$

where $G(v^{n+1}, v^n)_j$ has been defined in (2.21). We denote the SEPEWIFP discretization (7.11)-(7.12) for the oscillatory NLSW (7.6) as SEPEWIFPos.

Similar to Theorem 3.1, Lemma 3.3 and Theorem 4.1, we have the results about time symmetry, unique solvability and energy-preservation for the SEPEWIFPos method as follows.

Theorem 7.1. *The SEPEWIFPos method is time symmetric, i.e. interchanging* $u^{n+1}, \dot{u}^{n+1}$ *and* τ *with* $u^n, \dot{u}^n$ *and* $-\tau$*, respectively, the methods remain unchanged.*

Lemma 7.1 (Unique Solvability of SEPEWIFPos). *Given* v^n *and* $\dot{v}^n$ *with* $n \geq 0$*, there exists* v^{n+1} *and* $\dot{v}^{n+1}$ *satisfying the SEPEWIFPos method if* $k \neq 2q\alpha\varepsilon^\beta\pi$ *for arbitrary integer* q*. In addition, for sufficiently small values* $k_0 > 0$*, when* $0 < k \leq k_0$*, the solution is unique.*

Theorem 7.2. *The SEPEWIFPos method preserves exactly the energy in discrete level as*

$$\begin{aligned} E^n &:= \alpha\varepsilon^{2\beta}\|\dot{v}^n\|_{l^2}^2 + \big\|D_x v^n\big\|_{l^2}^2 + \varepsilon^2 h\sum_{j=0}^{M-1} F\big(\big|v_j^n\big|^2\big) \\ &\equiv \alpha\varepsilon^{2\beta}\|\dot{v}^0\|_{l^2}^2 + \big\|D_x v^0\big\|_{l^2}^2 + \varepsilon^2 h\sum_{j=0}^{M-1} F\big(\big|v_j^n\big|^2\big) := E^0, \quad n = 0, 1, \ldots. \end{aligned} \tag{7.13}$$

7.2. Convergence results

For our convergence analysis, we assume that the true solution of the NLSW (7.6) in the time interval $[0, T_0]$ satisfies

$$\begin{aligned} & v \in C\big([0,T_0]; H_p^{m_0+m}(\Omega)\big) \cap C^1\big([0,T_0]; H_p^{m+m_0-1}(\Omega)\big) \cap C^2\big([0,T_0]; H_p^m(\Omega)\big), \\ & \|\partial_s v(x,s)\|_{L^\infty([0,T_0];H_p^{m_0+m-1}(\Omega))} \lesssim \frac{1}{\varepsilon^\beta}, \quad \|\partial_{ss} v(x,s)\|_{L^\infty([0,T_0];H_p^m(\Omega))} \lesssim \frac{1}{\varepsilon^{2\beta}}, \\ & \|v(x,s)\|_{L^\infty([0,T_0];H_p^{m_0+m}(\Omega))} \lesssim 1, \end{aligned} \tag{B}$$

where $m_0 \geq 2, m > 1/2$. Define the errors as

$$e^n := v(x, s_n) - I_M v^n, \quad \dot{e}^n := \partial_s v(x, s_n) - I_M \dot{v}^n, \quad n = 0, 1, \dots, T_0/k \tag{7.14}$$

with approximations $v^n, \dot{v}^n \in X_M$ provided by the SEPEWIFPos method. Then we obtain error analysis results of the SEPEWIFPos method as follows.

Theorem 7.3. *Under the assumptions* (B)*, there exist sufficiently small constants $h_0 > 0$ and $k_0 > 0$ which are independent of ε and satisfy the conditions of Lemma* 7.1*, such that for any $0 < \varepsilon \leq 1$, when $0 < h \leq h_0$ and $0 < k \leq \varepsilon^{3\beta/2-1} k_0$, we obtain the error bounds for $0 \leq n \leq T_0/k$ as*

$$\begin{aligned} & \|e^n(x)\|_m \lesssim h^{m_0} + \varepsilon^{2-3\beta} k^2, && \|I_M v^n\|_m \leq 1 + M_v, \\ & \varepsilon^\beta \|\dot{e}^n(x)\|_{m-1} \lesssim h^{m_0} + \varepsilon^{2-3\beta} k^2, && \varepsilon^\beta \|I_M \dot{v}^n\|_{m-1} \leq 1 + M_v', \end{aligned} \tag{7.15}$$

where

$$\begin{aligned} & M_v := \|v(x,s)\|_{L^\infty([0,T_0];H^m(\Omega))}, \\ & M_v' := \|\partial_s v(x,s)\|_{L^\infty([0,T_0];H^{m-1}(\Omega))} \end{aligned}$$

When studying numerically oscillatory partial differential equations (PDEs) with a parameter ε, we often consider the ε-scalability of the method. The so called ε-scalability is that how the time step τ and mesh size h depend on the parameter ε. Theorem 7.3 means that the ε-scalability of the SEPEWIFPos method for the oscillatory NLSW (7.6) is

$$h = \mathcal{O}(1), \quad k = \mathcal{O}\left(\varepsilon^{\frac{3\beta}{2}-1}\sqrt{\delta_0}\right) = \mathcal{O}\left(\varepsilon^{\frac{3\beta}{2}-1}\right), \quad 0 \leq \beta \leq 2. \tag{7.16}$$

Remark 7.1. For the CNFD method which is also energy-preserving, we can take a very similar analysis for the NLSW (1.1) which has been taken for the oscillatory Klein-Gordon equations and Dirac equations [8, 18, 22] and conclude that the errors of CNFD methods are $\mathcal{O}(\varepsilon^{-\beta} h^2 + \varepsilon^{-3\beta}\tau^2)$ with $\beta \in [0, 2]$. That means that for CNFD, in order to obtain a reasonable numerical solution, we must take very small $\tau = \mathcal{O}(\varepsilon^{3\beta/2})$ and $h = \mathcal{O}(\varepsilon^{\beta/2})$, respectively. In contrast, our SEPEWIFPos method not only preserve the energy but also has the better ε-stability: $\tau = \mathcal{O}(\varepsilon^{3\beta/2-1})$ and $h = \mathcal{O}(1)$.

7.3. Numerical results of the oscillatory NLSW

To avoid repetitions, we consider the oscillatory NLSW (7.1) in the whole space $\mathbb{R}^d$. We only report numerical results with $d = 1$ to confirm the correctness of our theoretical analysis. Due to the fast decay of the solution at the far field, we truncate the original whole space problem onto a large enough bounded domain such as $\Omega = [-16, 16]$ with periodic boundary conditions. In the NLSW (7.1), we choose

$$u_0(x) = \mathrm{e}^{-x^2}, \quad u_1(x) = 2\mathrm{e}^{-x^2}, \quad x \in \Omega. \tag{7.17}$$

In order to describe the error, we take

$$\|e(\cdot, s_n)\|_m = \big\|v(\cdot, s_n) - v^n\big\|_m + \varepsilon^\beta \big\|v(\cdot, s_n) - v^n\big\|_{m-1},$$

where $v(x,s)$ and $\partial_s v(x,s)$ are the exact and its derivative, respectively. Here we only take m=1 as examples and do not consider $m \geq 2$ in that case the results are similar. We take the time intervals are $[0,1]$ and $\beta = 0, 4/3, 2$, respectively. Choosing $\beta = 4/3$ rather than $\beta = 1$ is to facilitate the selection of different ε and k. Tables 7.1-7.3 show the temporal errors of SEPEWIFPos method for different ε and k with $h = 1/16$. Table 7.4 shows the spatial errors of SEPEWIFPos method for different ε and h with $k = 10^{-4}$.

Next we will verify that this method is energy-preserving. In order to describe the long-term behavior of energy errors for the SEPEWIFPos method, we take the long enough time interval $[0, 1000]$, lager mesh size $h = 1$ and time step $\tau = 0.2$. In this case the error of the numerical solution tends to be large due to the long-term accumulation. The discrete energy are shown in Fig. 7.1. It should be noted that the minor errors appear in Fig. 7.1. The reason for this phenomenon has been explained in the previous sections.

In addition, with the same data, we also show long-term stability of the discrete mass of the SEPEWIFPos method in Fig. 7.2. Here we take the discrete mass as

$$M^n := \varepsilon^\beta \|v^n\|_{l^2}^2 - 2\varepsilon^{2\beta} h \sum_{j=0}^{M-1} \mathrm{Im}\big[\,\overline{v_j^n}\dot{v}_j^n\big], \quad n = 0, 1, \ldots, \tag{7.18}$$

where

$$\|v\|_{l^2}^2 = h \sum_{j=0}^{M-1} |v_j|^2.$$

Table 7.1: Temporal errors of the SEPEWIFPos method for different ε and k with $\beta = 0$.

$\|e(\cdot,1)\|_1$	$k_0 = 0.1$	$k_0/2$	$k_0/2^2$	$k_0/2^3$	$k_0/2^4$	$k_0/2^5$
$\varepsilon_0 = 1$	4.24E-3	1.07E-3	2.68E-4	6.69e-5	1.67e-5	4.18e-6
order	–	1.99	2.00	2.00	2.00	2.00
$\varepsilon_0/2$	7.42E-4	1.86E-4	4.66E-5	1.16E-5	2.91E-6	7.27E-7
order	–	1.99	2.00	2.00	2.00	2.00
$\varepsilon_0/2^2$	1.34E-4	3.36E-5	8.40E-6	2.10E-6	5.25E-7	1.31E-7
order	–	2.00	2.00	2.00	2.00	2.00
$\varepsilon_0/2^3$	2.82E-5	7.07E-6	1.77E-6	4.42E-7	1.10E-7	2.76E-8
order	–	2.00	2.00	2.00	2.00	2.00
$\varepsilon_0/2^4$	6.40E-6	1.60E-6	4.01E-7	1.00E-7	2.50E-8	6.26E-9
order	–	2.00	2.00	2.00	2.00	2.00
$\varepsilon_0/2^5$	1.50E-6	3.74E-7	9.36E-8	2.34E-8	5.85E-9	1.46E-9
order	–	2.00	2.00	2.00	2.00	2.00

Table 7.2: Temporal errors of the SEPEWIFPos method for different ε and k with $\beta = 4/3$.

$\|e(\cdot,1)\|_1$	$k_0 = 0.1$	$k_0/2$	$k_0/2^2$	$k_0/2^3$	$k_0/2^4$	$k_0/2^5$
$\varepsilon_0 = 1$	**4.24E-3**	1.07E-3	2.68E-4	6.69E-5	1.67E-5	4.18E-6
order	–	1.99	2.00	2.00	2.00	2.00
$\varepsilon_0/2$	9.17E-3	**2.33E-3**	5.85E-4	1.46E-4	3.66E-5	9.14E-6
order	–	**1.98**	1.99	2.00	2.00	2.00
$\varepsilon_0/2^2$	1.94E-2	5.13E-3	**1.30E-3**	3.27E-4	8.18E-5	2.04E-5
order	–	1.92	**1.98**	1.99	2.00	2.00
$\varepsilon_0/2^3$	3.90E-2	1.20E-2	3.21E-3	**8.15E-4**	2.05E-4	5.11E-5
order	–	1.70	1.91	**1.98**	1.99	2.00
$\varepsilon_0/2^4$	3.74E-2	2.32E-2	8.01E-3	2.21E-3	**5.66E-4**	1.42E-4
order	–	0.69	1.53	1.86	**1.96**	1.99
$\varepsilon_0/2^5$	1.82E-2	1.95E-2	1.54E-2	5.89E-3	1.67E-3	**4.33E-4**
order	–	-0.10	0.34	1.39	1.81	**1.95**

Table 7.3: Temporal errors of the SEPEWIFPos method for different ε and k with $\beta = 2$.

$\|e(\cdot,1)\|_1$	$k_0 = 0.1$	$k_0/2$	$k_0/2^2$	$k_0/2^3$	$k_0/2^4$	$k_0/2^5$
$\varepsilon_0 = 1$	**4.24E-3**	1.07E-3	2.68E-4	6.69E-5	1.67E-5	4.18E-6
order	–	1.99	2.00	2.00	2.00	2.00
$\varepsilon_0/\sqrt{2}$	8.45E-3	**2.14E-3**	5.37E-4	1.34E-4	3.36E-5	8.40E-6
order	–	**1.98**	2.00	2.00	2.00	2.00
$\varepsilon_0/\sqrt{2}^2$	2.09E-2	5.39E-3	**1.36E-3**	3.41E-4	8.52E-5	2.13E-5
order	–	1.95	**1.99**	2.00	2.00	2.00
$\varepsilon_0/\sqrt{2}^3$	5.13E-2	1.39E-2	3.56E-3	**4.24E-3**	8.96E-4	5.61E-5
order	–	1.88	1.97	**1.99**	2.00	2.00
$\varepsilon_0/\sqrt{2}^4$	1.23E-1	3.77E-2	1.00E-2	2.55E-3	**6.41E-4**	1.60E-4
order	–	1.71	1.91	1.98	**1.99**	2.00
$\varepsilon_0/\sqrt{2}^5$	1.88E-1	9.04E-2	2.76E-2	7.33E-3	1.86E-3	**4.67E-4**
order	–	1.06	1.71	1.91	1.98	**2.00**

From Tables 7.1-7.4 and Figs. 7.1-7.2, the following observations on the SEPEWIFPos method for the oscillatory NLSW (7.6) can be drawn:

(i) The temporal errors of the SEPEWIFPos method behave like $\mathcal{O}(\varepsilon^{2-3\beta}\tau^2)$ (see Tables 7.1-7.3).

(ii) The spatial errors of the SEPEWIFPos method are $\mathcal{O}(h^{m_0})$ which imply that the method is uniformly spectrally accurate for any $\varepsilon \in (0,1]$ and $\beta \in [0,2]$ (see each row in Table 7.4).

(iii) The discrete energy is preserved along the numerical solution of the SEPEWIFP method for the NLSW (7.6) (see Fig. 7.1). This verifies that the conclusion of Theorem 7.2 is correct.

(iv) Although this method does not preserve the discrete mass, it exhibits good long-term stability of the mass.

In summary, numerous numerical results strongly confirm the correctness of our theoretical analysis in this paper.

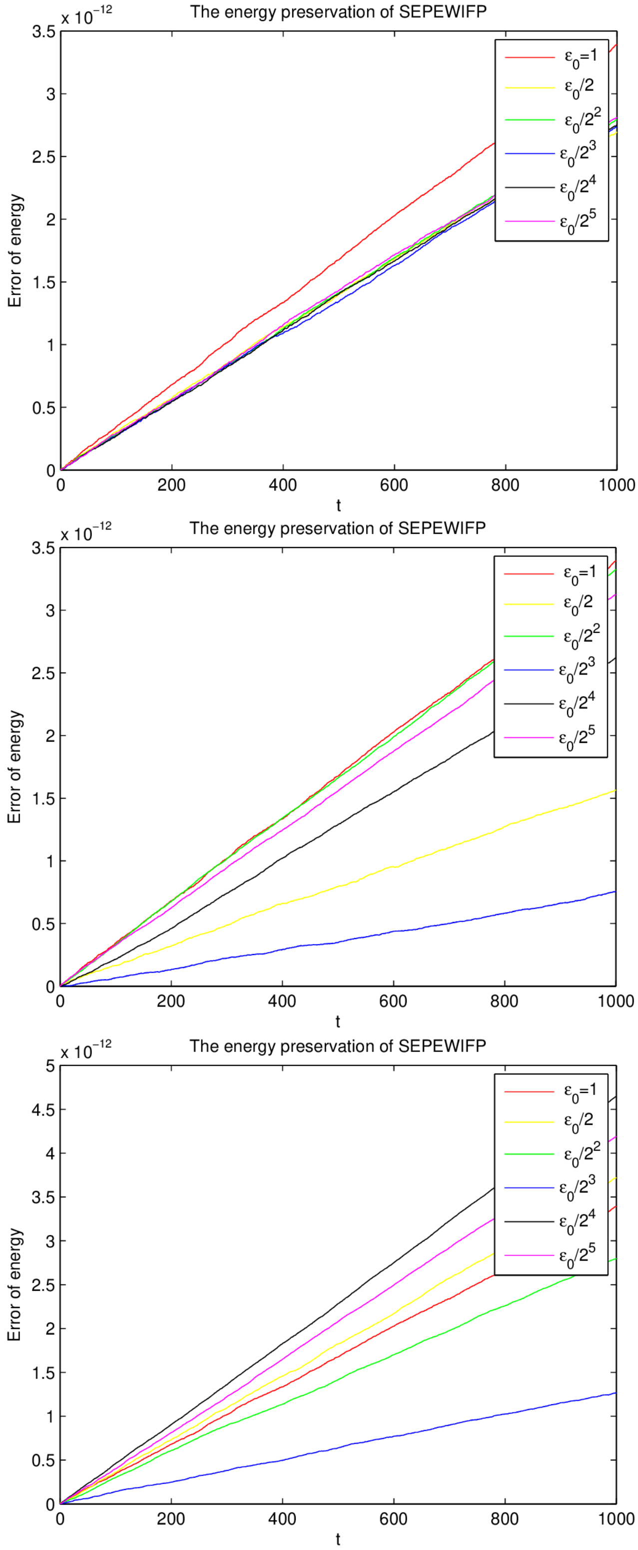

Fig. 7.1. Energy preservation for SEPEWIFPos with $\beta = 0, 1, 2$, respectively.

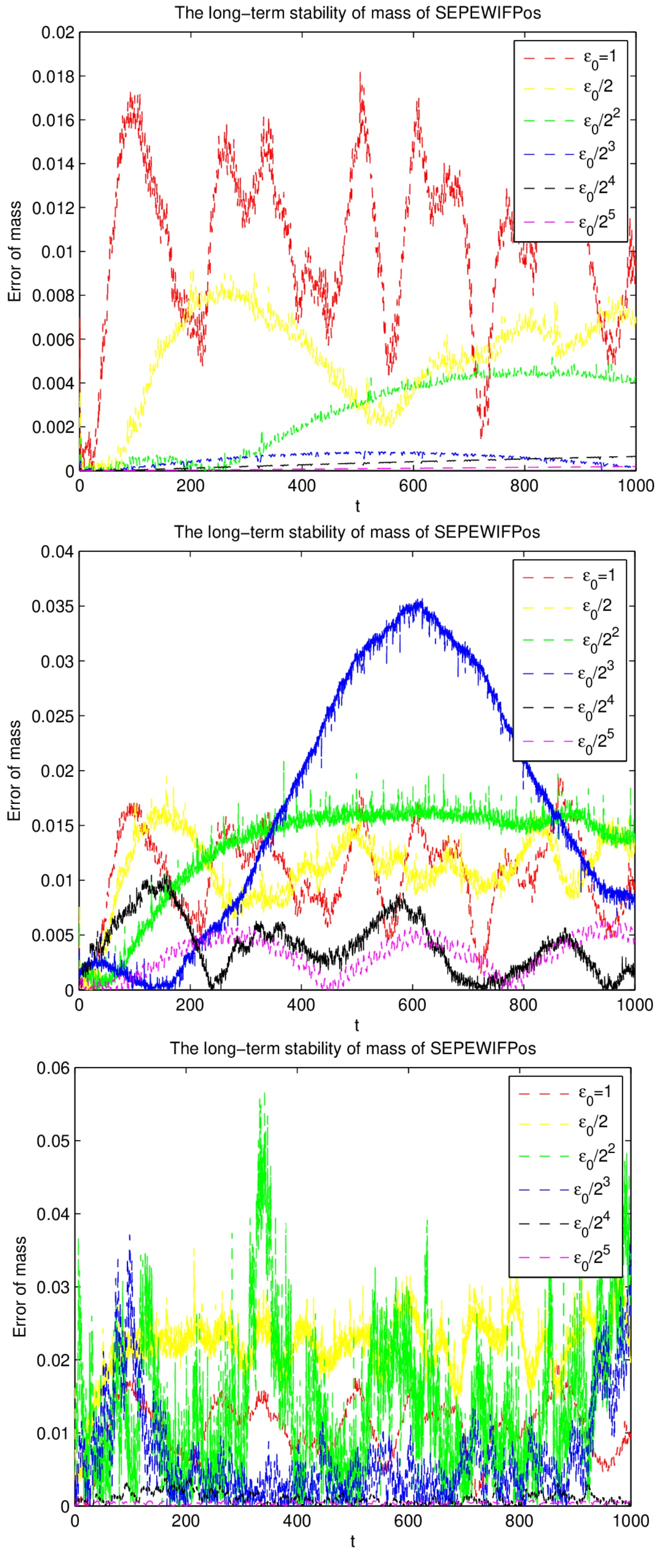

Fig. 7.2. Long-term stability of the mass for SEPEWIFPos with $\beta = 0, 1, 2$, respectively.

Table 7.4: Spatial errors of the SEPEWIFPos method for different ε and h with $\beta = 0, 1, 2$, respectively.

	$\|e(\cdot,1)\|_1$	$h_0 = 1$	$h_0/2$	$h_0/2^2$	$h_0/2^3$
$\beta = 0$	$\varepsilon_0 = 1$	5.46E-2	1.23E-3	6.90E-7	8.61E-13
	$\varepsilon_0/2$	3.13E-2	4.06E-4	2.86E-8	9.58E-13
	$\varepsilon_0/2^2$	2.71E-2	1.02E-4	2.42E-9	1.01E-12
	$\varepsilon_0/2^3$	2.68E-2	2.99E-5	3.08E-10	1.03E-12
	$\varepsilon_0/2^4$	2.67E-2	1.47E-5	5.82E-11	1.07E-12
$\beta = 1$	$\varepsilon_0 = 1$	5.46E-2	1.23E-3	6.90E-7	8.61E-13
	$\varepsilon_0/2$	5.34E-2	9.24E-4	1.89E-7	6.74E-13
	$\varepsilon_0/2^2$	5.40E-2	4.44E-4	3.98E-8	5.92E-13
	$\varepsilon_0/2^3$	5.12E-2	1.88E-4	8.14E-9	6.56E-13
	$\varepsilon_0/2^4$	2.67E-3	3.23E-5	1.24E-9	6.05E-13
$\beta = 2$	$\varepsilon_0 = 1$	5.46E-2	1.23E-3	6.90E-7	8.61E-13
	$\varepsilon_0/2$	7.14E-2	1.77E-3	9.96E-7	6.02E-13
	$\varepsilon_0/2^2$	8.33E-3	4.89E-4	2.15E-7	5.89E-13
	$\varepsilon_0/2^3$	2.90E-2	6.91E-5	6.17E-9	5.69E-13
	$\varepsilon_0/2^4$	5.01E-2	2.48E-5	1.18E-9	5.31E-13

8. Conclusions and Discussions

In this paper, we propose a time symmetric and energy-preserving exponential wave integrators Fourier pseudo-spectral (SEPEWIFP) method for the nonlinear Schrödinger equation (NLS) with wave operator (NLSW) and weak nonlinearity controlled by a small parameter $\varepsilon \in (0, 1]$. The new method is proved to be time symmetric and along the numerical solution, the discrete energy is preserved. By carrying out rigorous error estimates, we establish the uniform error bounds at $\mathcal{O}(h^{m_0} + \varepsilon^{2-\beta}\tau^2)$ up to the time at $\mathcal{O}(1/\varepsilon^\beta)$ for $\beta \in [0, 2]$ where h and τ are the mesh size and time step, respectively and m_0 depends on the regularity conditions. The tools for error analysis mainly include the cut-off technique to deal with the nonlinearity and the standard energy method. We also extend the results on error bounds, energy-preservation and time symmetry to the oscillatory NLSW with wavelength at $\mathcal{O}(\varepsilon^\beta)$ in time which is equivalent to the NLSW with weak nonlinearity. Specifically, the error bounds for the oscillatory NLSW are $\mathcal{O}(h^{m_0} + \varepsilon^{2-3\beta}k^2)$ and the ε-scalability is $h = \mathcal{O}(1)$ and $k = \mathcal{O}(\varepsilon^{3\beta/2-1})$ for $\beta \in [0, 2]$, where k is the time step. Numerical results confirm the correctness of our theoretical analysis. To the best of our knowledge there is no energy-preserving exponential wave integrator method for the NLSW.

Acknowledgements. The authors are grateful to the anonymous reviewers for their valuable suggestions, which help improve this paper significantly.

The research was supported in part by the Natural Science Foundation of Hebei Province (Grant No. A2021205036).

References

[1] G.D. Akrivis, Finite difference discretization of the cubic Schrödinger equation, *IMA J. Numer. Anal.*, **13**:1 (1993), 115–124.

[2] W. Bao and Y. Cai, Uniform error estimates of finite difference methods for the nonlinear Schrödinger equation with wave operator, *SIAM J. Numer. Anal.*, **50**:2 (2012), 492–521.

[3] W. Bao and Y. Cai, Mathematical theory and numerical methods for Bose-Einstein condensation, *Kinet. Relat. Models*, **6**:1 (2013), 1–135.

[4] W. Bao and Y. Cai, Optimal error estmiates of finite difference methods for the Gross-Pitaevskii equation with angular momentum rotation, *Math. Comp.*, **82**:281 (2013), 99–128.

[5] W. Bao and Y. Cai, Uniform and optimal error estimates of an exponential wave integrator sine pseudospectral method for the nonlinear Schrödinger equation with wave operator, *SIAM J. Numer. Anal.*, **52**:3 (2014), 1103–1127.

[6] W. Bao, X. Dong, and J. Xin, Comparisons between sine-Gordon and perturbed nonlinear Schrödinger equations for modeling light bullets beyond critical collapse, *Phys. D*, **239**:13 (2010), 1120–1134.

[7] W. Bao, Y. Feng, and C. Su, Uniform error bounds of time-splitting spectral methods for the long-time dynamics of the nonlinear Klein-Gordon equation with weak nonlinearity, *Math. Comp.*, **91** (2022), 811–842.

[8] W. Bao, Y. Feng, and W. Yi, Long time error analysis of finite difference time domain methods for the nonlinear Klein-Gordon equation with weak nonlinearity, *Commun. Comput. Phys.*, **26**:5 (2019), 1307–1334.

[9] W. Bao and C. Su, Uniform error bounds of a finite difference method for the Klein-Gordon-Zakharov system in the subsonic limit regime, *Math. Comp.*, **87**:313 (2018), 2133–2158.

[10] W. Bao, D. Jaksch, and P.A. Markowich, Numerical solution of the Gross-Pitaevskii equation for Bose-Einstein condensation, *J. Comput. Phys.*, **187**:1 (2003), 318–342.

[11] L. Bergé and T. Colin, A singular perturbation problem for an envelope equation in plasma physics, *Phys. D*, **84**:3-4 (1995), 437–459.

[12] C. Besse, B. Bidégaray, and S. Descombes, Order estimates in time of splitting methods for the nonlinear Schrödinger equation, *SIAM J. Numer. Anal.*, **40**:1 (2002), 26–40.

[13] Q. Chang, B. Guo, and H. Jiang, Finite difference method for generalized Zakharov equations, *Math. Comp.*, **64**:210 (1995), 537–553.

[14] X. Cheng, X. Yan, H. Qin, and H. Wang, Optimal l^∞ error estimates of the conservative scheme for two-dimensional Schrödinger equations with wave operator, *Comput. Math. Appl.*, **100** (2021), 74–82.

[15] T. Colin and P. Fabrie, Semidiscretization in time for nonlinear Schrödinger-waves equations, *Discrete Contin. Dyn. Syst.*, **4**:4 (1998), 671–690.

[16] A. Debussche and E. Faou, Modified energy for split-step methods applied to the linear Schrödinger equation, *SIAM J. Numer. Anal.*, **47**:5 (2009), 3705–3719.

[17] S. Deng and J. Li, A uniformly accurate exponential wave integrator Fourier pseudo-spectral method with energy-preservation for long-time dynamics of the nonlinear Klein-Gordon equation, *Appl. Numer. Math.*, **178** (2022), 166–191.

[18] Y. Feng, Long time error analysis of the fourth-order compact finite difference methods for the nonlinear Klein-Gordon equation with weak nonlinearity, *Numer. Methods Partial Differential Equations*, **37**:1 (2021), 897–914.

[19] Y. Feng, Y. Guo, and Y. Yuan, Uniform error bound of an exponential wave integrator for the long-time dynamics of the nonlinear Schrödinger equation with wave operator, *East Asian J. Appl. Math.*, **13**:4 (2023), 980–1003.

[20] Y. Feng, Z. Xu, and J. Yin, Uniform error bounds of exponential wave integrator methods for the long-time dynamics of the Dirac equation with small potentials, *Appl. Numer. Math.*, **172** (2022), 50–66.

[21] Y. Feng and W. Yi, Uniform error bounds of an exponential wave integrator for the long-time dynamics of the nonlinear Klein-Gordon equation, *Multiscale Model. Simul.*, **19**:3 (2021), 1212–1235.

[22] Y. Feng and J. Yin, Spatial resolution of different discretizations over long-time for the Dirac equation with small potentials, *J. Comput. Appl. Math.*, **412** (2022), 114342.

[23] B. Guo and H. Liang, On the problem of numerical calculation for a class of systems of nonlinear Schrödinger equations with wave operator, *J. Numer. Methods Comput. Appl.*, **4** (1983), 176–182.

[24] Y. Guo, *Multiscale Methods and Analysis for the Nonlinear Schrödinger Equation with Wave Operator*, PhD Thesis, National University of Singapore, 2021.

[25] E. Hairer, C. Lubich, and G. Wanner, *Geometric Numerical Integration: Structure-Preserving Algorithms for Ordinary Differential Equations*, Springer, 2006.

[26] R.H. Hardin and F.D. Tappert, Applications of the split-step Fourier method to the numerical solution of nonlinear and variable coefficient wave equations, *SIAM Rev.*, **15** (1973), 423.

[27] S. Klainerman, Global existence of small amplitude solutions to nonlinear Klein-Gordon equations in four space-time dimensions, *Comm. Pure Appl. Math.*, **38**:5 (1985), 631–641.

[28] S. Labidi and K. Omrani, A new conservative fourth-order accurate difference scheme for the nonlinear Schrödinger equation with wave operator, *Appl. Numer. Math.*, **173** (2022), 1–12.

[29] J. Li, Energy-preserving exponential integrator Fourier pseudo-spectral schemes for the nonlinear Dirac equation, *Appl. Numer. Math.*, **172** (2022), 1–26.

[30] J. Li and H. Fang, Improved uniform error bounds of a time-splitting Fourier pseudo-spectral method for the Klein-Gordon-Schrödinger equation with the small coupling constant, *Math. Comput. Simulation*, **212** (2023), 267–288.

[31] J. Li and X. Jin, Structure-preserving exponential wave integrator methods and the long-time convergence analysis for the Klein-Gordon-Dirac equation with the small coupling constant, *Numer. Methods Partial Differential Equations*, **39**:4 (2023), 3375–3416.

[32] J. Li and L. Zhu, A uniformly accurate exponential wave integrator Fourier pseudo-spectral method with structure-preservation for long-time dynamics of the Dirac equation,with small potentials, *Numer. Algorithms*, **92** (2023), 1367–1401.

[33] C. Lubich, On splitting methods for Schrödinger-Poisson and cubic nonlinear Schrödinger equations, *Math. Comp.*, **77** (2008), 2141–2153.

[34] S. Machihara, K. Nakanishi, and T. Ozawa, Nonrelativistic limit in the energy space for nonlinear Klein-Gordon equations, *Math. Ann.*, **322** (2002), 603–621.

[35] A.Y. Schoene, On the nonrelativistic limits of the Klein-Gordon and Dirac equations, *J. Math. Anal. Appl.*, **71**:1 (1979), 36–47.

[36] J. Shen, T. Tang, and L. Wang, *Spectral Methods: Algorithms, Analysis and Applications*, Springer, 2011.

[37] M. Tsutumi, Nonrelativistic approximation of nonlinear Klein-Gordon equations in two space dimensions, *Nonlinear Anal.*, **8**:6 (1984), 637–643.

[38] T. Wang and L. Zhang, Analysis of some new conservative schemes for nonlinear Schrödinger equation with wave operator, *Appl. Math. Comput.*, **182**:2 (2006), 1780–1794.

[39] J. Xin, Modeling light bullets with the two-dimensional sine-Gordon equation, *Phys. D*, **135**:3-4 (2000), 345–368.

[40] X. Zhao, A combination of multiscale time integrator and two-scale formulation for the nonlinear Schrödinger equation with wave operator, *J. Comput. Appl. Math.*, **326** (2017), 320–336.